(7) De Francesco, R.; Migliaccio, G. Challenges and successes in developing new therapies for hepatitis C. *Nature* **2005**, *436* (7053), 953–60.
(8) Kato, N.; Mori, K.; Abe, K.; Dansako, H.; Kuroki, M.; Ariumi, Y.; Wakita, T.; Ikeda, M. Efficient replication systems for hepatitis C virus using a new human hepatoma cell line. *Virus Res.* **2009**, *146* (1–2), 41–50.
(9) Murray, C. L.; Rice, C. M. Hepatitis C: An unsuspected drug target. *Nature* **2010**, *465* (7294), 42–4.
(10) Mori, Y.; Moriishi, K.; Matsuura, Y. Hepatitis C virus core protein: its coordinate roles with PA28gamma in metabolic abnormality and carcinogenicity in the liver. *Int. J. Biochem. Cell Biol.* **2008**, *40* (8), 1437–42.
(11) Gao, G.; Luo, H. The ubiquitin-proteasome pathway in viral infections. *Can. J. Physiol. Pharmacol.* **2006**, *84* (1), 5–14.
(12) Miyamoto, H.; Moriishi, K.; Moriya, K.; Murata, S.; Tanaka, K.; Suzuki, T.; Miyamura, T.; Koike, K.; Matsuura, Y. Involvement of the PA28gamma-dependent pathway in insulin resistance induced by hepatitis C virus core protein. *J. Virol.* **2007**, *81* (4), 1727–35.
(13) Moriishi, K.; Okabayashi, T.; Nakai, K.; Moriya, K.; Koike, K.; Murata, S.; Chiba, T.; Tanaka, K.; Suzuki, R.; Suzuki, T.; Miyamura, T.; Matsuura, Y. Proteasome activator PA28gamma-dependent nuclear retention and degradation of hepatitis C virus core protein. *J. Virol.* **2003**, *77* (19), 10237–49.
(14) Moriishi, K.; Shoji, I.; Mori, Y.; Suzuki, R.; Suzuki, T.; Kataoka, C.; Matsuura, Y. Involvement of PA28gamma in the propagation of hepatitis C virus. *Hepatology* **2010**, *52* (2), 411–20.
(15) Suzuki, R.; Moriishi, K.; Fukuda, K.; Shirakura, M.; Ishii, K.; Shoji, I.; Wakita, T.; Miyamura, T.; Matsuura, Y.; Suzuki, T. Proteasomal turnover of hepatitis C virus core protein is regulated by two distinct mechanisms: a ubiquitin-dependent mechanism and a ubiquitin-independent but PA28gamma-dependent mechanism. *J. Virol.* **2009**, *83* (5), 2389–92.
(16) Chen, Y. A.; Tripathi, L. P.; Mizuguchi, K. TargetMine, an integrated data warehouse for candidate gene prioritisation and target discovery. *PLoS One* **2011**, *6* (3), e17844.
(17) Liu, M. C.; Akle, V.; Zheng, W.; Dave, J. R.; Tortella, F. C.; Hayes, R. L.; Wang, K. K. Comparing calpain- and caspase-3-mediated degradation patterns in traumatic brain injury by differential proteome analysis. *Biochem. J.* **2006**, *394* (Pt 3), 715–25.
(18) Stark, C.; Breitkreutz, B. J.; Reguly, T.; Boucher, L.; Breitkreutz, A.; Tyers, M. BioGRID: a general repository for interaction datasets. *Nucleic Acids Res.* **2006**, *34* (Database issue), D535–9.
(19) Turner, B.; Razick, S.; Turinsky, A. L.; Vlasblom, J.; Crowdy, E. K.; Cho, E.; Morrison, K.; Donaldson, I. M.; Wodak, S. J. iRefWeb: interactive analysis of consolidated protein interaction data and their supporting evidence. *Database (Oxford)* **2010**, *2010*, baq023.
(20) Cline, M. S.; Smoot, M.; Cerami, E.; Kuchinsky, A.; Landys, N.; Workman, C.; Christmas, R.; Avila-Campilo, I.; Creech, M.; Gross, B.; Hanspers, K.; Isserlin, R.; Kelley, R.; Killcoyne, S.; Lotia, S.; Maere, S.; Morris, J.; Ono, K.; Pavlovic, V.; Pico, A. R.; Vailaya, A.; Wang, P. L.; Adler, A.; Conklin, B. R.; Hood, L.; Kuiper, M.; Sander, C.; Schmulevich, I.; Schwikowski, B.; Warner, G. J.; Ideker, T.; Bader, G. D. Integration of biological networks and gene expression data using Cytoscape. *Nat. Protoc.* **2007**, *2* (10), 2366–82.
(21) Assenov, Y.; Ramirez, F.; Schelhorn, S. E.; Lengauer, T.; Albrecht, M. Computing topological parameters of biological networks. *Bioinformatics* **2008**, *24* (2), 282–4.
(22) Tripathi, L. P.; Kataoka, C.; Taguwa, S.; Moriishi, K.; Mori, Y.; Matsuura, Y.; Mizuguchi, K. Network based analysis of hepatitis C virus Core and NS4B protein interactions. *Mol. Biosyst.* **2010**, *6* (12), 2539–53.
(23) Ashburner, M.; Ball, C. A.; Blake, J. A.; Botstein, D.; Butler, H.; Cherry, J. M.; Davis, A. P.; Dolinski, K.; Dwight, S. S.; Eppig, J. T.; Harris, M. A.; Hill, D. P.; Issel-Tarver, L.; Kasarskis, A.; Lewis, S.; Matese, J. C.; Richardson, J. E.; Ringwald, M.; Rubin, G. M.; Sherlock, G. Gene ontology: tool for the unification of biology. The Gene Ontology Consortium. *Nat. Genet.* **2000**, *25* (1), 25–9.
(24) Aoki-Kinoshita, K. F.; Kanehisa, M. Gene annotation and pathway mapping in KEGG. *Methods Mol. Biol.* **2007**, *396*, 71–91.
(25) McKusick-Nathans Institute of Genetic Medicine, Johns Hopkins Medicine (Baltimore, MD) and National Center for Biotechnology Information, National Library of Medicine (Bethesda, MD), Online Mendelian Inheritance in Man, OMIM (TM). In 2010.
(26) Benjamini, Y.; Hochberg, Y. Controlling the false discovery rate-A practical and powerful approach to multiple testing. *J. R. Statist. Soc. B* **1995**, *57* (1), 289–300.
(27) Noble, W. S. How does multiple testing correction work? *Nat. Biotechnol.* **2009**, *27* (12), 1135–7.
(28) Linhart, C.; Halperin, Y.; Shamir, R. Transcription factor and microRNA motif discovery: the Amadeus platform and a compendium of metazoan target sets. *Genome Res.* **2008**, *18* (7), 1180–9.
(29) Montgomery, S. B.; Griffith, O. L.; Sleumer, M. C.; Bergman, C. M.; Bilenky, M.; Pleasance, E. D.; Prychyna, Y.; Zhang, X.; Jones, S. J. ORegAnno: an open access database and curation system for literature-derived promoters, transcription factor binding sites and regulatory variation. *Bioinformatics* **2006**, *22* (5), 637–40.
(30) Okamoto, T.; Omori, H.; Kaname, Y.; Abe, T.; Nishimura, Y.; Suzuki, T.; Miyamura, T.; Yoshimori, T.; Moriishi, K.; Matsuura, Y. A single-amino-acid mutation in hepatitis C virus NS5A disrupting FKBP8 interaction impairs viral replication. *J. Virol.* **2008**, *82* (7), 3480–9.
(31) Pietschmann, T.; Lohmann, V.; Kaul, A.; Krieger, N.; Rinck, G.; Rutter, G.; Strand, D.; Bartenschlager, R. Persistent and transient replication of full-length hepatitis C virus genomes in cell culture. *J. Virol.* **2002**, *76* (8), 4008–21.
(32) Kato, T.; Date, T.; Miyamoto, M.; Furusaka, A.; Tokushige, K.; Mizokami, M.; Wakita, T. Efficient replication of the genotype 2a hepatitis C virus subgenomic replicon. *Gastroenterology* **2003**, *125* (6), 1808–17.
(33) Wakita, T.; Pietschmann, T.; Kato, T.; Date, T.; Miyamoto, M.; Zhao, Z.; Murthy, K.; Habermann, A.; Krausslich, H. G.; Mizokami, M.; Bartenschlager, R.; Liang, T. J. Production of infectious hepatitis C virus in tissue culture from a cloned viral genome. *Nat. Med.* **2005**, *11* (7), 791–6.
(34) Cao, W.; Sun, B.; Feitelson, M. A.; Wu, T.; Tur-Kaspa, R.; Fan, Q. Hepatitis C virus targets over-expression of arginase I in hepatocarcinogenesis. *Int. J. Cancer* **2009**, *124* (12), 2886–92.
(35) Tacke, R. S.; Tosello-Trampont, A.; Nguyen, V.; Mullins, D. W.; Hahn, Y. S. Extracellular hepatitis C virus core protein activates STAT3 in human monocyte/macrophage/dendritic cells via an IL-6 autocrine pathway. *J. Biol. Chem.* **2011**, DOI: 10.1074/jbc.M110.217653 .
(36) Waris, G.; Turkson, J.; Hassanein, T.; Siddiqui, A. Hepatitis C virus (HCV) constitutively activates STAT-3 via oxidative stress: role of STAT-3 in HCV replication. *J. Virol.* **2005**, *79* (3), 1569–80.
(37) Randall, G.; Panis, M.; Cooper, J. D.; Tellinghuisen, T. L.; Sukhodolets, K. E.; Pfeffer, S.; Landthaler, M.; Landgraf, P.; Kan, S.; Lindenbach, B. D.; Chien, M.; Weir, D. B.; Russo, J. J.; Ju, J.; Brownstein, M. J.; Sheridan, R.; Sander, C.; Zavolan, M.; Tuschl, T.; Rice, C. M. Cellular cofactors affecting hepatitis C virus infection and replication. *Proc. Natl. Acad. Sci. U.S.A.* **2007**, *104* (31), 12884–9.
(38) Lin, W.; Kim, S. S.; Yeung, E.; Kamegaya, Y.; Blackard, J. T.; Kim, K. A.; Holtzman, M. J.; Chung, R. T. Hepatitis C virus core protein blocks interferon signaling by interaction with the STAT1 SH2 domain. *J. Virol.* **2006**, *80* (18), 9226–35.
(39) Tsutsumi, T.; Suzuki, T.; Moriya, K.; Shintani, Y.; Fujie, H.; Miyoshi, H.; Matsuura, Y.; Koike, K.; Miyamura, T. Hepatitis C virus core protein activates ERK and p38 MAPK in cooperation with ethanol in transgenic mice. *Hepatology* **2003**, *38* (4), 820–8.
(40) Nanda, S. K.; Herion, D.; Liang, T. J. The SH3 binding motif of HCV [corrected] NS5A protein interacts with Bin1 and is important for apoptosis and infectivity. *Gastroenterology* **2006**, *130* (3), 794–809.
(41) Jacobs, J. M.; Diamond, D. L.; Chan, E. Y.; Gritsenko, M. A.; Qian, W.; Stastna, M.; Baas, T.; Camp, D. G., 2nd; Carithers, R. L., Jr.; Smith, R. D.; Katze, M. G. Proteome analysis of liver cells expressing a full-length hepatitis C virus (HCV) replicon and biopsy specimens of

posttransplantation liver from HCV-infected patients. *J. Virol.* **2005**, *79* (12), 7558–69.
(42) Woodhouse, S. D.; Narayan, R.; Latham, S.; Lee, S.; Antrobus, R.; Gangadharan, B.; Luo, S.; Schroth, G. P.; Klenerman, P.; Zitzmann, N. Transcriptome sequencing, microarray, and proteomic analyses reveal cellular and metabolic impact of hepatitis C virus infection in vitro. *Hepatology* **2010**, *52* (2), 443–53.
(43) Fujino, T.; Nakamuta, M.; Yada, R.; Aoyagi, Y.; Yasutake, K.; Kohjima, M.; Fukuizumi, K.; Yoshimoto, T.; Harada, N.; Yada, M.; Kato, M.; Kotoh, K.; Taketomi, A.; Maehara, Y.; Nakashima, M.; Enjoji, M. Expression profile of lipid metabolism-associated genes in hepatitis C virus-infected human liver. *Hepatol. Res.* **2010**, *40* (9), 923–9.
(44) MacPherson, J. I.; Sidders, B.; Wieland, S.; Zhong, J.; Targett-Adams, P.; Lohmann, V.; Backes, P.; Delpuech-Adams, O.; Chisari, F.; Lewis, M.; Parkinson, T.; Robertson, D. L. An integrated transcriptomic and meta-analysis of hepatoma cells reveals factors that influence susceptibility to HCV infection. *PLoS One* **2011**, *6* (10), e25584.
(45) de Chassey, B.; Navratil, V.; Tafforeau, L.; Hiet, M. S.; Aublin-Gex, A.; Agaugue, S.; Meiffren, G.; Pradezynski, F.; Faria, B. F.; Chantier, T.; Le Breton, M.; Pellet, J.; Davoust, N.; Mangeot, P. E.; Chaboud, A.; Penin, F.; Jacob, Y.; Vidalain, P. O.; Vidal, M.; Andre, P.; Rabourdin-Combe, C.; Lotteau, V. Hepatitis C virus infection protein network. *Mol. Syst. Biol.* **2008**, *4*, 230.
(46) Chazal, N.; Gerlier, D. Virus entry, assembly, budding, and membrane rafts. *Microbiol. Mol. Biol. Rev.* **2003**, *67* (2), 226–37.
(47) Manes, S.; del Real, G.; Martinez, A. C. Pathogens: raft hijackers. *Nat. Rev. Immunol.* **2003**, *3* (7), 557–68.
(48) Riethmuller, J.; Riehle, A.; Grassme, H.; Gulbins, E. Membrane rafts in host-pathogen interactions. *Biochim. Biophys. Acta* **2006**, *1758* (12), 2139–47.
(49) Suzuki, T.; Suzuki, Y. Virus infection and lipid rafts. *Biol. Pharm. Bull.* **2006**, *29* (8), 1538–41.
(50) Mannova, P.; Fang, R.; Wang, H.; Deng, B.; McIntosh, M. W.; Hanash, S. M.; Beretta, L. Modification of host lipid raft proteome upon hepatitis C virus replication. *Mol. Cell. Proteomics* **2006**, *5* (12), 2319–25.
(51) Corless, L.; Crump, C. M.; Griffin, S. D.; Harris, M. Vps4 and the ESCRT-III complex are required for the release of infectious hepatitis C virus particles. *J. Gen. Virol.* **2010**, *91* (Pt 2), 362–72.
(52) Lai, C. K.; Jeng, K. S.; Machida, K.; Lai, M. M. Hepatitis C virus egress and release depend on endosomal trafficking of core protein. *J. Virol.* **2010**, *84* (21), 11590–8.
(53) Jahn, R.; Scheller, R. H. SNAREs—engines for membrane fusion. *Nat. Rev. Mol. Cell. Biol.* **2006**, *7* (9), 631–43.
(54) Kreykenbohm, V.; Wenzel, D.; Antonin, W.; Atlachkine, V.; von Mollard, G. F. The SNAREs vti1a and vti1b have distinct localization and SNARE complex partners. *Eur. J. Cell Biol.* **2002**, *81* (5), 273–80.
(55) Kunwar, A. J.; Rickmann, M.; Backofen, B.; Browski, S. M.; Rosenbusch, J.; Schoning, S.; Fleischmann, T.; Krieglstein, K.; Fischer von Mollard, G. Lack of the endosomal SNAREs vti1a and vti1b led to significant impairments in neuronal development. *Proc. Natl. Acad. Sci. U.S.A.* **2011**, *108* (6), 2575–80.
(56) Mascia, L.; Langosch, D. Evidence that late-endosomal SNARE multimerization complex is promoted by transmembrane segments. *Biochim. Biophys. Acta* **2007**, *1768* (3), 457–66.
(57) Offenhauser, C.; Lei, N.; Roy, S.; Collins, B. M.; Stow, J. L.; Murray, R. Z. Syntaxin 11 binds Vti1b and regulates late endosome to lysosome fusion in macrophages. *Traffic* **2011**, *12*, 762–73.
(58) Bryceson, Y. T.; Chiang, S. C.; Darmanin, S.; Fauriat, C.; Schlums, H.; Theorell, J.; Wood, S. M. Molecular mechanisms of natural killer cell activation. *J. Innate Immun.* **2011**, *3* (3), 216–26.
(59) Arneson, L. N.; Brickshawana, A.; Segovis, C. M.; Schoon, R. A.; Dick, C. J.; Leibson, P. J. Cutting edge: syntaxin 11 regulates lymphocyte-mediated secretion and cytotoxicity. *J. Immunol.* **2007**, *179* (6), 3397–401.
(60) Dabrazhynetskaya, A.; Ma, J.; Guerreiro-Cacais, A. O.; Arany, Z.; Rudd, E.; Henter, J. I.; Karre, K.; Levitskaya, J.; Levitsky, V. Syntaxin 11 marks a distinct intracellular compartment recruited to the immunological synapse of NK cells to co-localize with cytotoxic granules. *J. Cell. Mol. Med.* **2011**, *16*, 129–41.
(61) Gholam, C.; Grigoriadou, S.; Gilmour, K. C.; Gaspar, H. B. Familial haemophagocytic lymphohistiocytosis: advances in the genetic basis, diagnosis and management. *Clin. Exp. Immunol.* **2011**, *163* (3), 271–83.
(62) How, P. C.; Shields, D. Tethering function of the caspase cleavage fragment of Golgi protein p115 promotes apoptosis via a p53-dependent pathway. *J. Biol. Chem.* **2011**, *286* (10), 8565–76.
(63) Radulescu, A. E.; Mukherjee, S.; Shields, D. The Golgi protein p115 associates with gamma-tubulin and plays a role in Golgi structure and mitosis progression. *J. Biol. Chem.* **2011**, *286* (24), 21915–26.
(64) Bouffard, P.; Hayashi, P. H.; Acevedo, R.; Levy, N.; Zeldis, J. B. Hepatitis C virus is detected in a monocyte/macrophage subpopulation of peripheral blood mononuclear cells of infected patients. *J. Infect. Dis.* **1992**, *166* (6), 1276–80.
(65) Roxrud, I.; Raiborg, C.; Pedersen, N. M.; Stang, E.; Stenmark, H. An endosomally localized isoform of Eps15 interacts with Hrs to mediate degradation of epidermal growth factor receptor. *J. Cell Biol.* **2008**, *180* (6), 1205–18.
(66) Salcini, A. E.; Chen, H.; Iannolo, G.; De Camilli, P.; Di Fiore, P. P. Epidermal growth factor pathway substrate 15, Eps15. *Int. J. Biochem. Cell Biol.* **1999**, *31* (8), 805–9.
(67) Barnaba, V. Hepatitis C virus infection: a "liaison a trois" amongst the virus, the host, and chronic low-level inflammation for human survival. *J. Hepatol.* **2010**, *53* (4), 752–61.
(68) Hiroishi, K.; Ito, T.; Imawari, M. Immune responses in hepatitis C virus infection and mechanisms of hepatitis C virus persistence. *J. Gastroenterol. Hepatol.* **2008**, *23* (10), 1473–82.
(69) Kawai, T.; Akira, S. Toll-like receptor and RIG-I-like receptor signaling. *Ann. N.Y. Acad. Sci.* **2008**, *1143*, 1–20.
(70) Sklan, E. H.; Charuworn, P.; Pang, P. S.; Glenn, J. S. Mechanisms of HCV survival in the host. *Nat. Rev. Gastroenterol. Hepatol.* **2009**, *6* (4), 217–27.
(71) Szabo, G.; Dolganiuc, A. Hepatitis C and innate immunity: recent advances. *Clin. Liver Dis.* **2008**, *12* (3), 675–92.
(72) Taylor, D. R.; Silberstein, E. Innate immunity and hepatitis C virus: eluding the host cell defense. *Front. Biosci.* **2009**, *14*, 4950–61.
(73) Legarda-Addison, D.; Hase, H.; O'Donnell, M. A.; Ting, A. T. NEMO/IKKgamma regulates an early NF-kappaB-independent cell-death checkpoint during TNF signaling. *Cell Death Differ.* **2009**, *16* (9), 1279–88.
(74) Ye, X.; Lu, H.; Huo, K.; Chen, D. Finding a novel interacting protein of the hepatic carcinoma related gene MIP: NF-kappaB essential modulator (NEMO). *Oncol. Rep.* **2011**, *25* (1), 231–5.
(75) Beraza, N.; Malato, Y.; Sander, L. E.; Al-Masaoudi, M.; Freimuth, J.; Riethmacher, D.; Gores, G. J.; Roskams, T.; Liedtke, C.; Trautwein, C. Hepatocyte-specific NEMO deletion promotes NK/NKT cell- and TRAIL-dependent liver damage. *J. Exp. Med.* **2009**, *206* (8), 1727–37.
(76) Cruz-Munoz, M. E.; Veillette, A. Do NK cells always need a license to kill? *Nat. Immunol.* **2010**, *11* (4), 279–80.
(77) Wang, K.; Song, Y.; Chen, D. B.; Zheng, J. Protein phosphatase 3 differentially modulates vascular endothelial growth factor- and fibroblast growth factor 2-stimulated cell proliferation and signaling in ovine fetoplacental artery endothelial cells. *Biol. Reprod.* **2008**, *79* (4), 704–10.
(78) Singh, A. P.; Bafna, S.; Chaudhary, K.; Venkatraman, G.; Smith, L.; Eudy, J. D.; Johansson, S. L.; Lin, M. F.; Batra, S. K. Genome-wide expression profiling reveals transcriptomic variation and perturbed gene networks in androgen-dependent and androgen-independent prostate cancer cells. *Cancer Lett.* **2008**, *259* (1), 28–38.
(79) Ostenfeld, M. S.; Bramsen, J. B.; Lamy, P.; Villadsen, S. B.; Fristrup, N.; Sorensen, K. D.; Ulhoi, B.; Borre, M.; Kjems, J.; Dyrskjot, L.; Orntoft, T. F. miR-145 induces caspase-dependent and -independent cell death in urothelial cancer cell lines with targeting of an expression signature present in Ta bladder tumors. *Oncogene* **2010**, *29* (7), 1073–84.

(80) Johansen, C.; Vestergaard, C.; Kragballe, K.; Kollias, G.; Gaestel, M.; Iversen, L. MK2 regulates the early stages of skin tumor promotion. *Carcinogenesis* **2009**, *30* (12), 2100–8.
(81) Wang, C.; Zhou, J.; Wang, S.; Ye, M.; Fan, G.; Zou, H.; Jiang, C. Shotgun approach based comparative proteomic analysis of levo-tetrahydropalmatine-induced apoptosis in hepatocytes. *Toxicol. Lett.* **2010**, *194* (1–2), 8–15.
(82) Del Campo, J. A.; Romero-Gomez, M. Steatosis and insulin resistance in hepatitis C: a way out for the virus? *World J. Gastroenterol.* **2009**, *15* (40), 5014–9.
(83) Douglas, M. W.; George, J. Molecular mechanisms of insulin resistance in chronic hepatitis C. *World J. Gastroenterol.* **2009**, *15* (35), 4356–64.
(84) Shintani, Y.; Fujie, H.; Miyoshi, H.; Tsutsumi, T.; Tsukamoto, K.; Kimura, S.; Moriya, K.; Koike, K. Hepatitis C virus infection and diabetes: direct involvement of the virus in the development of insulin resistance. *Gastroenterology* **2004**, *126* (3), 840–8.
(85) Cao, X.; Pobezinskaya, Y. L.; Morgan, M. J.; Liu, Z. G. The role of TRADD in TRAIL-induced apoptosis and signaling. *FASEB J.* **2011**, *25* (4), 1353–8.
(86) Zheng, L.; Bidere, N.; Staudt, D.; Cubre, A.; Orenstein, J.; Chan, F. K.; Lenardo, M. Competitive control of independent programs of tumor necrosis factor receptor-induced cell death by TRADD and RIP1. *Mol. Cell. Biol.* **2006**, *26* (9), 3505–13.
(87) Tellinghuisen, T. L.; Foss, K. L.; Treadaway, J. Regulation of hepatitis C virion production via phosphorylation of the NS5A protein. *PLoS Pathog.* **2008**, *4* (3), e1000032.
(88) Benedicto, I.; Molina-Jimenez, F.; Bartosch, B.; Cosset, F. L.; Lavillette, D.; Prieto, J.; Moreno-Otero, R.; Valenzuela-Fernandez, A.; Aldabe, R.; Lopez-Cabrera, M.; Majano, P. L. The tight junction-associated protein occludin is required for a postbinding step in hepatitis C virus entry and infection. *J. Virol.* **2009**, *83* (16), 8012–20.
(89) Bantel, H.; Schulze-Osthoff, K. Apoptosis in hepatitis C virus infection. *Cell Death Differ.* **2003**, *10* (Suppl 1), S48–58.
(90) Deng, L.; Adachi, T.; Kitayama, K.; Bungyoku, Y.; Kitazawa, S.; Ishido, S.; Shoji, I.; Hotta, H. Hepatitis C virus infection induces apoptosis through a Bax-triggered, mitochondrion-mediated, caspase 3-dependent pathway. *J. Virol.* **2008**, *82* (21), 10375–85.
(91) Fischer, R.; Baumert, T.; Blum, H. E. Hepatitis C virus infection and apoptosis. *World J. Gastroenterol.* **2007**, *13* (36), 4865–72.
(92) Hanafy, S. M.; Shehata, O. H.; Farahat, N. M. Expression of apoptotic markers BCL-2 and Bax in chronic hepatitis C virus patients. *Clin. Biochem.* **2010**, *43* (13–14), 1112–7.
(93) Joyce, M. A.; Walters, K. A.; Lamb, S. E.; Yeh, M. M.; Zhu, L. F.; Kneteman, N.; Doyle, J. S.; Katze, M. G.; Tyrrell, D. L. HCV induces oxidative and ER stress, and sensitizes infected cells to apoptosis in SCID/Alb-uPA mice. *PLoS Pathog.* **2009**, *5* (2), e1000291.
(94) Kondo, Y.; Machida, K.; Liu, H. M.; Ueno, Y.; Kobayashi, K.; Wakita, T.; Shimosegawa, T.; Lai, M. M. Hepatitis C virus infection of T cells inhibits proliferation and enhances fas-mediated apoptosis by down-regulating the expression of CD44 splicing variant 6. *J. Infect. Dis.* **2009**, *199* (5), 726–36.
(95) Anupam, R.; Datta, A.; Kesic, M.; Green-Church, K.; Shkriabai, N.; Kvaratskhelia, M.; Lairmore, M. D. Human T-lymphotropic virus type 1 p30 interacts with REGgamma and modulates ATM (ataxia telangiectasia mutated) to promote cell survival. *J. Biol. Chem.* **2011**, *286* (9), 7661–8.
(96) Mao, I.; Liu, J.; Li, X.; Luo, H. REGgamma, a proteasome activator and beyond? *Cell. Mol. Life Sci.* **2008**, *65* (24), 3971–80.
(97) Tian, M.; Xiaoyi, W.; Xiaotao, L.; Guosheng, R. Proteasomes reactivator REG gamma enchances oncogenicity of MDA-MB-231 cell line via promoting cell proliferation and inhibiting apoptosis. *Cell. Mol. Biol. (Noisy-le-Grand)* **2009**, *55* (Suppl), OL1121–31.
(98) Zannini, L.; Buscemi, G.; Fontanella, E.; Lisanti, S.; Delia, D. REGgamma/PA28gamma proteasome activator interacts with PML and Chk2 and affects PML nuclear bodies number. *Cell Cycle* **2009**, *8* (15), 2399–407.
(99) Samuelsen, J. T.; Schwarze, P. E.; Huitfeldt, H. S.; Thrane, E. V.; Lag, M.; Refsnes, M.; Skarpen, E.; Becher, R. Regulation of rat alveolar type 2 cell proliferation in vitro involves type II cAMP-dependent protein kinase. *Am. J. Physiol. Lung Cell. Mol. Physiol.* **2007**, *292* (1), L232–9.
(100) Bungyoku, Y.; Shoji, I.; Makine, T.; Adachi, T.; Hayashida, K.; Nagano-Fujii, M.; Ide, Y. H.; Deng, L.; Hotta, H. Efficient production of infectious hepatitis C virus with adaptive mutations in cultured hepatoma cells. *J. Gen. Virol.* **2009**, *90* (Pt 7), 1681–91.
(101) Lemon, S. M.; McKeating, J. A.; Pietschmann, T.; Frick, D. N.; Glenn, J. S.; Tellinghuisen, T. L.; Symons, J.; Furman, P. A. Development of novel therapies for hepatitis C. *Antiviral Res.* **2010**, *86* (1), 79–92.
(102) Lin, K. Development of novel antiviral therapies for hepatitis C virus. *Virol. Sin.* **2010**, *25* (4), 246–66.
(103) Chan, S. C.; Lo, S. Y.; Liou, J. W.; Lin, M. C.; Syu, C. L.; Lai, M. J.; Chen, Y. C.; Li, H. C. Visualization of the structures of the hepatitis C virus replication complex. *Biochem. Biophys. Res. Commun.* **2011**, *404* (1), 574–8.
(104) Dreyer, J. L. Lentiviral vector-mediated gene transfer and RNA silencing technology in neuronal dysfunctions. *Mol. Biotechnol.* **2011**, *47* (2), 169–87.
(105) Camm, E. J.; Martin-Gronert, M. S.; Wright, N. L.; Hansell, J. A.; Ozanne, S. E.; Giussani, D. A. Prenatal hypoxia independent of undernutrition promotes molecular markers of insulin resistance in adult offspring. *FASEB J.* **2011**, *25* (1), 420–7.
(106) Ning, B. F.; Ding, J.; Yin, C.; Zhong, W.; Wu, K.; Zeng, X.; Yang, W.; Chen, Y. X.; Zhang, J. P.; Zhang, X.; Wang, H. Y.; Xie, W. F. Hepatocyte nuclear factor 4 alpha suppresses the development of hepatocellular carcinoma. *Cancer Res.* **2010**, *70* (19), 7640–51.
(107) Niehof, M.; Borlak, J. EPS15R, TASP1, and PRPF3 are novel disease candidate genes targeted by HNF4alpha splice variants in hepatocellular carcinomas. *Gastroenterology* **2008**, *134* (4), 1191–202.
(108) Hussain, K. M.; Leong, K. L.; Ng, M. M.; Chu, J. J. The essential role of clathrin-mediated endocytosis in the infectious entry of human enterovirus 71. *J. Biol. Chem.* **2011**, *286* (1), 309–21.
(109) Helle, F.; Dubuisson, J. Hepatitis C virus entry into host cells. *Cell. Mol. Life Sci.* **2008**, *65* (1), 100–12.
(110) Marshall, A.; Rushbrook, S.; Morris, L. S.; Scott, I. S.; Vowler, S. L.; Davies, S. E.; Coleman, N.; Alexander, G. Hepatocyte expression of minichromosome maintenance protein-2 predicts fibrosis progression after transplantation for chronic hepatitis C virus: a pilot study. *Liver Transpl.* **2005**, *11* (4), 427–33.
(111) Bard-Chapeau, E. A.; Li, S.; Ding, J.; Zhang, S. S.; Zhu, H. H.; Princen, F.; Fang, D. D.; Han, T.; Bailly-Maitre, B.; Poli, V.; Varki, N. M.; Wang, H.; Feng, G. S. Ptpn11/Shp2 acts as a tumor suppressor in hepatocellular carcinogenesis. *Cancer Cell* **2011**, *19* (5), 629–39.
(112) Matsuo, K.; Delibegovic, M.; Matsuo, I.; Nagata, N.; Liu, S.; Bettaieb, A.; Xi, Y.; Araki, K.; Yang, W.; Kahn, B. B.; Neel, B. G.; Haj, F. G. Altered glucose homeostasis in mice with liver-specific deletion of Src homology phosphatase 2. *J. Biol. Chem.* **2010**, *285* (51), 39750–8.
(113) Rios, E. J.; Piliponsky, A. M.; Ra, C.; Kalesnikoff, J.; Galli, S. J. Rabaptin-5 regulates receptor expression and functional activation in mast cells. *Blood* **2008**, *112* (10), 4148–57.
(114) Stenmark, H.; Vitale, G.; Ullrich, O.; Zerial, M. Rabaptin-5 is a direct effector of the small GTPase Rab5 in endocytic membrane fusion. *Cell* **1995**, *83* (3), 423–32.
(115) Edamoto, Y.; Hara, A.; Biernat, W.; Terracciano, L.; Cathomas, G.; Riehle, H. M.; Matsuda, M.; Fujii, H.; Scoazec, J. Y.; Ohgaki, H. Alterations of RB1, p53 and Wnt pathways in hepatocellular carcinomas associated with hepatitis C, hepatitis B and alcoholic liver cirrhosis. *Int. J. Cancer* **2003**, *106* (3), 334–41.
(116) Laurent-Puig, P.; Zucman-Rossi, J. Genetics of hepatocellular tumors. *Oncogene* **2006**, *25* (27), 3778–86.
(117) Park, K. J.; Choi, S. H.; Koh, M. S.; Kim, D. J.; Yie, S. W.; Lee, S. Y.; Hwang, S. B. Hepatitis C virus core protein potentiates c-Jun N-terminal kinase activation through a signaling complex involving TRADD and TRAF2. *Virus Res.* **2001**, *74* (1–2), 89–98.
(118) Kawaguchi, T.; Yoshida, T.; Harada, M.; Hisamoto, T.; Nagao, Y.; Ide, T.; Taniguchi, E.; Kumemura, H.; Hanada, S.; Maeyama, M.;

Baba, S.; Koga, H.; Kumashiro, R.; Ueno, T.; Ogata, H.; Yoshimura, A.; Sata, M. Hepatitis C virus down-regulates insulin receptor substrates 1 and 2 through up-regulation of suppressor of cytokine signaling 3. *Am. J. Pathol.* **2004**, *165* (5), 1499–508.

(119) Ma, Z.; Liu, Z.; Wu, R. F.; Terada, L. S. p66(Shc) restrains Ras hyperactivation and suppresses metastatic behavior. *Oncogene* **2010**, *29* (41), 5559–67.

(120) Spoden, G. A.; Rostek, U.; Lechner, S.; Mitterberger, M.; Mazurek, S.; Zwerschke, W. Pyruvate kinase isoenzyme M2 is a glycolytic sensor differentially regulating cell proliferation, cell size and apoptotic cell death dependent on glucose supply. *Exp. Cell Res.* **2009**, *315* (16), 2765–74.

# Upregulation of nuclear PA28γ expression in cirrhosis and hepatocellular carcinoma

MOTOI KONDO[1], KOHJI MORIISHI[2], HIROSHI WADA[3], TAKEHIRO NODA[3], SHIGERU MARUBASHI[3], KENICHI WAKASA[4], YOSHIHARU MATSUURA[2], YUICHIRO DOKI[3], MASAKI MORI[3] and HIROAKI NAGANO[3]

[1]Evidence Based Medical Research Center, Osaka; [2]Department of Molecular Virology, Research Institute for Microbial Diseases, Osaka University, Osaka; [3]Department of Gastroenterological Surgery, Graduate School of Medicine, Osaka University, Osaka; [4]Department of Diagnostic Pathology, Graduate School of Medicine, Osaka City University, Osaka, Japan

Received September 16, 2011; Accepted December 2, 2011

DOI: 10.3892/etm.2011.415

**Abstract.** We previously reported that proteasome activator 28γ (PA28γ) is an oncogenic protein in hepatitis C virus (HCV) core protein transgenic mice. The aim of this study was to determine the role of PA28γ expression at the protein level in the development and progression of human hepatocarcinogenesis and hepatocellular carcinoma (HCC). Samples from tissues representing a wide spectrum of liver disease were analyzed, including histologically normal livers (n=5), HCV-related chronic hepatitis (CH) (n=15) and cirrhosis (n=31). The level of nuclear PA28γ increased with the progression of liver disease from CH to cirrhosis. The majority of cirrhotic livers (68%; 21/31) displayed high nuclear PA28γ expression. However, in half of the HCCs (50%; 18/36), little or no nuclear PA28γ expression was observed, while the remaining 50% (18/36) of the cases displayed high levels of nuclear PA28γ expression. A clinicopathological survey demonstrated a significant correlation between nuclear PA28γ expression and capsular invasion in HCC (P=0.026); a striking difference was found between nuclear PA28γ expression in non-tumor tissues and shorter disease-free survival (P<0.01). Moreover, nuclear PA28γ expression in non-tumor tissues correlated with the expression of molecules related to the genesis of hepatic steatosis and HCC, such as sterol regulatory element binding protein-1c mRNA. The findings suggest the involvement of nuclear PA28γ expression in the progression and relapse of HCC, and suggest that nuclear PA28γ is a potentially suitable target for the prevention and/or treatment of HCC.

*Correspondence to:* Dr Hiroaki Nagano, Department of Gastroenterological Surgery, Graduate School of Medicine, Osaka University, 2-2 Yamadaoka E-2, Suita, Osaka 565-0871, Japan
E-mail: hnagano@gesurg.med.osaka-u.ac.jp

*Abbreviations:* CH, chronic hepatitis; HBV, hepatitis B virus; HCC, hepatocellular carcinoma; HCV, hepatitis C virus; PA, proteasome activator; PBGD, porphobilinogen deaminase; RT-PCR, reverse transcription-polymerase chain reaction

*Key words:* proteasome activator 28γ, hepatocellular carcinoma, cirrhosis, western blotting, immunohistochemistry

## Introduction

Hepatocellular carcinoma (HCC) is one of the most common malignancies worldwide, accounting for approximately 6% of all human carcinomas and 1 million deaths annually, with an estimated number of new cases of over 500,000/year (1). Clinical and experimental evidence suggests a link between infection with hepatitis C virus (HCV) and/or hepatitis B virus (HBV), chronic hepatitis (CH) and cirrhosis, as well as the progression of HCC. Liver cirrhosis is observed in up to 90% of patients with HCC, and HCV is the causative factor in 80% and HBV in 10% of cases in Japan (2-5). In the United States, almost 4 million individuals are infected with HCV each year which progresses to chronic hepatitis C, which could potentially progress to liver cirrhosis. The results are often liver failure or HCC. Chronic hepatitis C is the nation's leading cause of HCC, and according to the American Liver Foundation, is also the leading reason for liver transplantation. In Japan, HCV and/or HBV-based hepatitis and cirrhosis are also serious problems since they progress to HCC at a ratio of 5 to 7% per year (4,5). These findings strongly suggest the existence of a link between hepatocarcinogenesis and HCV/HBV infection and chronic liver inflammation.

Various therapies are currently in use for HCC. These include surgical resection, percutaneous ethanol injection (PEI), systemic or arterial chemotherapy using either single or combination drugs, transcatheter arterial chemoembolization (TACE), hormonal therapy and selective radiotherapy. However, the prognosis of patients with HCC remains poor, as they often develop intrahepatic and/or multicentric tumor recurrence, at a rate of 20-40% within 1 year, and ~80% within 5 years of therapy even when curative treatment is applied (6-9). Liver transplantation offers the best prognosis for patients with small HCC, although its use is limited due to the scarcity of donor organs. Therefore, an effective therapeutic strategy against HCC is required.

In a previous study, we reported that proteasome activator 28γ (PA28γ) directly enhances the degradation of the HCV core protein and plays a key role in the genesis of hepatic steatosis and HCC in HCV core protein transgenic mice (10). Furthermore, the above events were not observed in PA28γ-knockout mice. The present study is an extension of our previous study and was designed to assess the utility of PA28γ expression as a biological marker for HCV-related human liver disease and HCC. The findings showed the presence of high levels of nuclear PA28γ in multistep hepatocarcinogenesis and HCC invasion, suggesting that selective inhibitors of nuclear PA28γ may be useful in the prevention and/or treatment of this disease.

## Materials and methods

*Tissue samples*. The study protocol was approved by the Human Ethics Review Committee of Osaka University, and a signed consent form was obtained from each subject for the use of tissue samples for medical research. Tissue samples were obtained from 51 patients with liver tumors, who underwent hepatectomy at the Department of Gastroenterological Surgery, Osaka University Hospital. All patients had HCV infection (28 patients) and some had HCV plus HBV infection (18 patients), but none had only HBV infection. The mean post-treatment follow-up period was 6.2±2.5 years ± standard deviation (SD). The excised hepatic tissue samples were examined immunohistochemically for PA28γ expression, including 46 paired HCCs. Non-tumor tissues were also examined, which comprised 15 CH-based livers (5 chronic active hepatitis and 10 chronic inactive hepatitis) and 31 cirrhotic livers. Prior to hepatectomy for HCC, 10 patients were treated with transarterial embolization (TAE). In these cases, histopathological examination showed complete hepatic necrosis. Histologically normal livers were also obtained from patients negative for hepatic viral infections who had liver metastasis secondary to colorectal cancer.

For immunohistochemistry, the tissue samples were fixed in 10% neutral buffered formalin, processed through graded ethanol and embedded in paraffin. The samples were frozen immediately in liquid nitrogen and stored at -80°C for subsequent analysis by reverse transcription-polymerase chain reaction (RT-PCR).

*Histopathological examination*. Tissue sections (4 μm thick) were deparaffinized in xylene, rehydrated and stained with hematoxylin and eosin solution. Separation of the tissues into non-tumor and tumor tissues was determined by a pathologist (K.W.) who was blinded to the clinical background. For non-tumor tissues, the presence of inflammation or cirrhotic nodules was examined. Tumor tissues were examined for the following characteristics: cell differentiation (well, moderate, poorly differentiated), number of tumors, capsular formation, septal formation, capsular invasion, portal vein tumor thrombus formation and hepatic vein invasion.

*Preparation of anti-human PA28γ antibody*. Chicken anti-human PA28γ antibody was prepared by immunization using the synthetic peptides of residues from 75 to 88, SHDGLDGPTYKKRR, of human PA28γ. The antibody was purified by affinity chromatography using beads conjugated with the antigen peptide.

*Immunohistochemistry and evaluation of PA28γ immunostaining*. Formalin-fixed tissues were embedded in paraffin according to the standard procedures. For immunohistochemistry, formalin-fixed tissue sections were boiled in Target Retrieval Solution (Dako, Glostrup, Denmark) and then treated with 3% $H_2O_2$. The activated sections were washed twice with phosphate-buffered saline (PBS), blocked with PBS containing 5% bovine serum albumin, and incubated overnight with the purified chicken antibody to PA28γ, followed by incubation with horseradish peroxidase-conjugated anti-chicken IgG antibody (ICN, Biomedicals, Inc., Aurora, OH, USA) as a secondary antibody. Immunoreactive antigen was visualized with 3,3'-diaminobenzidine substrate. The resulting sections were counterstained with hematoxylin. Staining of endogenous PA28γ with the antibody was identified in normal mouse liver sections but not in the liver sections from PA28γ-deficient mice. Pre-immune purified antibody did not react with any other antigen in these sections under the experimental conditions.

For evaluation of PA28γ immunostaining, each section was scored for nuclear and cytoplasmic staining using a scale from 0 to 2 where 0 represented negative or faint staining, 1 represented moderate staining, and 2 represented strong staining. In general, the nuclei of the bile ducts faintly expressed PA28γ (Fig. 1a). Thus, the staining level was used as a nuclear inner control within the sample, which was designated arbitrarily as intensity level 0. Also, slightly higher expression was designated arbitrarily as intensity level 1 and clearly higher expression was designated arbitrarily as intensity level 2. PA28γ expression was very faint or undetectable in the vascular epithelia and nuclei (Fig. 1a), whereas the cytoplasm of bile duct epithelial cells and nuclei devoid of significant inflammation generally expressed faint levels of PA28γ (Fig. 1a). For semi-quantitative analysis, the latter level of staining was used as a cytoplasmic inner control within the sample, and designated arbitrarily as intensity level 0. Furthermore, a slightly higher expression was designated arbitrarily as intensity level 1 whereas clearly higher expression was designated arbitrarily as intensity level 2. PA28γ expression was generally heterogeneous in each sample. For assessment of nuclear and cytoplasmic PA28γ, 4 high-power fields in each specimen were selected at random, and staining was examined under high power magnification. More than 1,000 cells were counted to determine the labeling index, which represented the percentage of immunostained cells relative to the total number of cells. The tissue samples were also categorized as positive (levels 1 and 2) and negative (level 0) for evaluation of the relationship between immunostaining and various clinicopathological factors.

*Semi-quantitative RT-PCR*. RNA extraction was carried out with TRIzol reagent using the single-step method, and the cDNA was generated with avian myeloblastosis virus reverse transcriptase (Promega, Madison, WI, USA), as described previously (11). Sterol regulatory element binding protein-1c (SREBP-1c) mRNA expression was analyzed semi-quantitatively using the multiplex RT-PCR method. In this assay, the

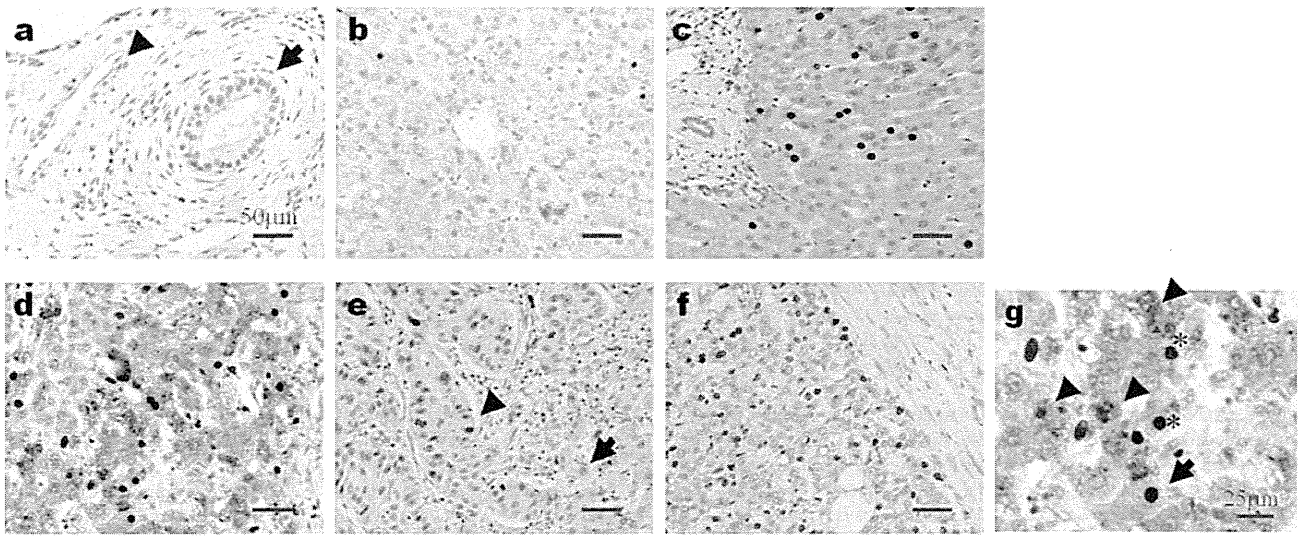


Figure 1. Immunohistochemical staining for PA28γ. (a-f) Representative samples for bile duct (inner control), vascular epithelium and various liver pathologies; (a) bile duct (arrow), vascular epithelium (arrowhead); (b) normal liver; (c) chronic hepatitis; (d) cirrhotic liver; (e) HCC with high nuclear PA28γ expression (arrowhead; left side) and non-tumor liver tissue with low nuclear PA28γ expression (arrow; right side); (f) HCC with low expression of nuclear PA28γ. Magnification, x200. (g) High-power view of liver section shown in (d). Note the faint staining of hepatocytes with high expression of nuclear PA28γ (arrow; hepatocytes, level 0 and nucleus, level 2), moderate staining of hepatocytes with high expression of nuclear PA28γ (asterisk; hepatocyte, level 1 and nucleus, level 2) and strong staining of hepatocytes with low expression of nuclear PA28γ (arrowhead; hepatocyte, level 2 and nucleus, level 0). Magnification, x400. No staining was observed when the primary antibody was substituted by non-immunized rabbit IgG or TBS (data not shown). PA28γ, proteasome activator 28γ; HCC, hepatocellular carcinoma; IgG, immunoglobulin G; TBS, Tris-buffered saline.

housekeeping gene, porphobilinogen deaminase (PBGD), was used as the internal control. This gene is favored over β-actin or glyceraldehyde-3-phosphate dehydrogenase as a reference gene for competitive PCR amplification as the presence of pseudogenes for the latter housekeeping genes may produce false-positive signals from genomic DNA contamination (12,13). In addition, in order to minimize possible inter-PCR differences, PCR was performed with SREBP-1c and PBGD primers in an identical tube, under unsaturated conditions. PCR was performed in a 25-$\mu$l reaction mixture containing 1 $\mu$l of the cDNA template, 1X Perkin-Elmer PCR buffer, 1.5 mM $MgCl_2$, 0.8 mM deoxynucleotide triphosphates, 0.8 $\mu$M of each primer for SREBP-1c and 80 nM PBGD, and 1 unit of TaqDNA polymerase (AmpliTaq Gold; Roche Molecular Systems, Inc.). The PCR primers used for the detection of SREBP-1c and PBGD cDNAs were synthesized as described previously (14,15). The conditions for multiplex PCR were one cycle of denaturation at 95˚C for 12 min, followed by 40 cycles at 95˚C for 1 min, 62˚C for 1 min and 72˚C for 1 min, and a final extension at 72˚C for 10 min. The electrophoresed PCR products were scanned by densitometry, and the relative value of the SREBP-1c band relative to that of PBGD was calculated for each sample.

*Statistical analysis*. Data were expressed as the means ± SD. The Chi-square test and Fisher's exact probability test, or the log-rank test, were used to examine the association between PA28γ expression and the clinicopathological parameters or prognosis. A P-value of <0.05 was considered to indicate a statistically significant difference. Statistical analysis was performed using the StatView-J-5.0 program (SAS Institute, Cary, NC, USA).

## Results

*Immunohistochemical analysis of PA28γ*. Immunohistochemical assays were performed on a series of 46 paired HCCs and their matched non-tumor tissues, and 5 normal livers. The labeling index of nuclear PA28γ showed a wide spectrum and increased from low in the normal livers to strong in the cirrhotic livers (Fig. 1b-d). Specifically, the nuclear PA28γ labeling index was generally low in the normal liver tissues, but was moderate-strong in HCV-related liver tissues. The nuclear labeling index was markedly higher in the majority of cirrhotic liver tissues. Fig. 2 summarizes the above results and the analysis of cytoplasmic expression of PA28γ. The difference in the PA28γ-nuclear labeling index between normal and cirrhotic livers was significant (P<0.0001) as was that between CH and cirrhosis (P<0.0001) (Fig. 2A). Also, the difference in the proportion of the PA28γ-cytoplasmic expression labeling index between normal and cirrhotic livers was significant (P<0.05) (Fig. 2B). The mean labeling indexes of nuclear PA28γ expression was 42% in both HCC and HCV-related livers.

To evaluate the relationship between immunohistochemical staining and various clinicopathological factors, we divided the samples into nuclear PA28γ high index (≥42%) and low index (<42%) groups. The labeling index was low in half of the examined HCC cases (50%; 18/36) and markedly high in the other half (50%; 18/36) (Table I). The labeling index was low in 30% (14/46) of HCV-related cases and markedly higher in the remaining 70% (32/46) (Table II). The samples were also divided into 2 groups according to the labeling index of cytoplasmic staining. The mean PA28γ-labeling index of the HCC and HCV-related cases was 58 and 80%, respectively. The labeling index was low in 47% (17/36) and high in 53% (19/36)

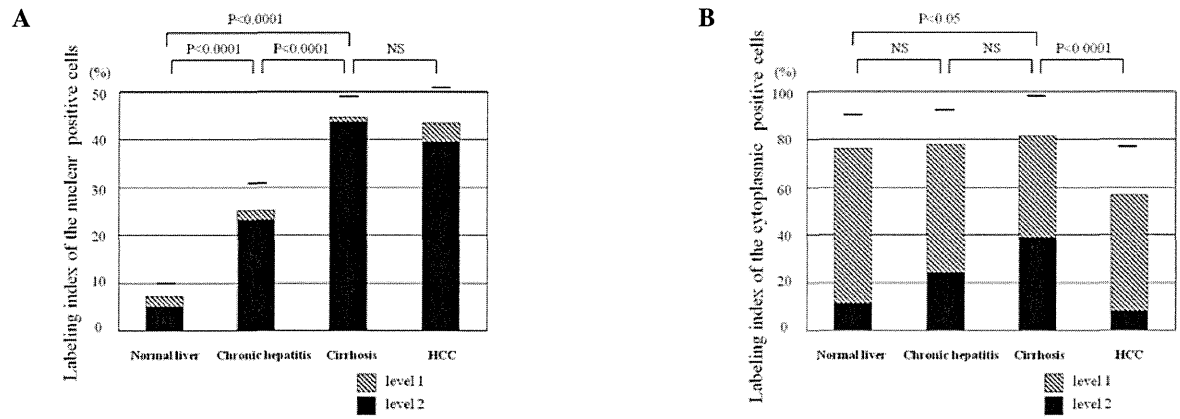


Figure 2. (A) Nuclear PA28γ expression in multistep hepatocarcinogenesis. The labeling index increased in a stepwise manner with the severity of liver damage and carcinogenesis. Quantitative analysis showed that 25, 10 and 1% of cells of the normal liver, CH and cirrhosis, respectively, were moderately positive (level 1). In HCCs, 10% of cells were evaluated as moderately positive (level 1). (B) Cytoplasmic PA28γ expression in multistep hepatocarcinogenesis. The expression increased slightly in a stepwise manner. Quantitative analysis showed that 80, 68 and 50% of cells of the normal liver, CH and cirrhosis, respectively, were moderately positive (level 1). In HCCs, 82% of cells were evaluated as moderately positive (level 1). PA28γ, proteasome activator 28γ; CH, chronic hepatitis; HCC, hepatocellular carcinoma. NS, not significant.

Table I. Correlation between nuclear PA28γ expression and various clinicopathological parameters in patients with HCC.

| | | PA28γ | | |
|---|---|---|---|---|
| | n | Low (<42%) | High (≥42%) | P-value |
| Age (years) | | | | |
| ≥60 | 15 | 7 | 8 | |
| <60 | 21 | 11 | 10 | NS |
| Gender | | | | |
| Male | 21 | 10 | 11 | |
| Female | 15 | 8 | 7 | NS |
| Tumor size | | | | |
| ≤2 cm | 8 | 4 | 4 | |
| >2 cm | 28 | 14 | 14 | NS |
| Histological type | | | | |
| Well/moderately differentiated | 5 | 2 | 3 | |
| Poorly differentiated | 31 | 16 | 15 | NS |
| Hepatic vein invasion | | | | |
| Yes | 6 | 2 | 4 | |
| No | 30 | 16 | 14 | NS |
| Portal vein tumor thrombus | | | | |
| Yes | 5 | 2 | 3 | |
| No | 31 | 16 | 15 | NS |
| Number of tumors | | | | |
| Multiple[a] | 3 | 1 | 2 | |
| Solitary | 33 | 17 | 16 | NS |
| Septum formation | | | | |
| Yes | 15 | 8 | 7 | |
| No | 21 | 10 | 11 | NS |
| Capsular formation | | | | |
| Yes | 14 | 6 | 8 | |
| No | 22 | 12 | 10 | NS |
| Capsular invasion | | | | |
| Yes | 8 | 1 | 7 | |
| No | 6 | 5 | 1 | 0.026 |

[a]This category includes intrahepatic metastasis and multicentric carcinogenesis. PA28γ, proteasome activator 28γ; HCC, hepatocellular carcinoma; NS, not significant.

Table II. Correlation between nuclear PA28γ expression and various clinicopathological parameters in non-tumor liver tissues.

| | n | PA28γ | | P-value |
|---|---|---|---|---|
| | | Low (<42%) | High (≥42%) | |
| Age (years) | | | | |
| ≥60 | 22 | 5 | 17 | |
| <60 | 24 | 9 | 15 | NS |
| Gender | | | | |
| Male | 27 | 6 | 21 | |
| Female | 19 | 8 | 11 | NS |
| HCV | 28 | 9 | 19 | |
| HBV | 0 | | | |
| HCV plus HBV | 18 | 5 | 13 | NS |
| Inflammatory status (HAI score) | | | | |
| Absent-mild (0-3) | 22 | 12 | 10 | |
| Moderate-severe (>4) | 24 | 2 | 22 | 0.0007 |
| Degree of fibrosis (HAI score) | | | | |
| Absent-moderate (0-2) | 12 | 11 | 1 | |
| Severe-cirrhosis (>3) | 34 | 3 | 31 | <0.0001 |

NS, not significant; PA28γ, proteasome activator 28γ; HCV, hepatitis C virus; HBV, hepatitis B virus; HAI, histological activity index.

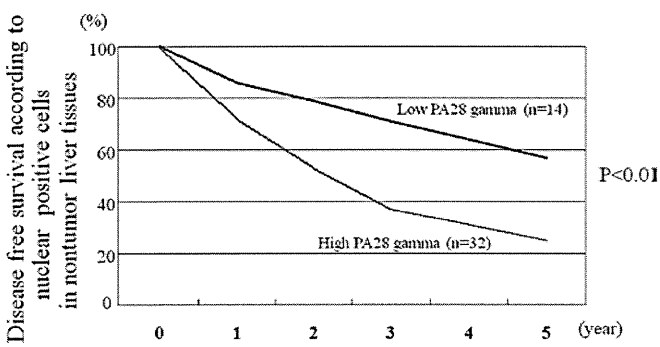


Figure 3. Disease-free survival based on nuclear PA28γ expression in non-tumor tissues. The disease-free survival was significantly different between patients with high nuclear PA28γ expression (levels 1 and 2) and those with low nuclear PA28γ expression (level 0) (P<0.01). PA28γ, proteasome activator 28γ.

of the HCC cases. The respective values for HCV-related cases were 28% (13/46) and 72% (33/46). All cut-off values used were according to the mean labeling index.

*Correlation between nuclear PA28γ expression and clinicopathological parameters.* We examined the correlation between PA28γ nuclear expression analyzed in 36 HCCs (10 samples with complete necrosis by TAE were excluded from this analysis) and various clinicopathological features (Table I). The cases were divided into two groups based on the labeling index of nuclear expression of PA28γ, using a cut-off mean value of 42%. There was a significant difference in PA28γ expression based on capsular invasion (Table I). We also analyzed the relationship between nuclear PA28γ expression in non-tumor tissues (15 CH and 31 cirrhosis) and disease-free survival, as the pathologic status of non-tumor tissues has been shown to correlate with the relapse of HCC (16-18). The disease-free survival, but not overall survival (P=0.052), was significantly different between high and low nuclear PA28γ expressors (P<0.01) (Fig. 3). In addition, PA28γ expression in non-tumor tissues correlated closely with active inflammation and fibrosis (Table II).

In univariate analysis, PA28γ expression in non-tumor liver tissues, portal vein tumor thrombus, inflammatory status and degree of fibrosis in the non-cancerous liver tissue were significant factors for disease-free survival. These variables were subsequently entered into multivariate analysis. The results identified nuclear PA28γ expression level [95% confidence interval (CI), 1.82-3.22; P<0.01], portal vein tumor thrombus (95% CI, 1.33-6.38; P=0.023), inflammatory status (95% CI, 2.11-3.58; P=0.012) and degree of fibrosis (95% CI, 1.99-7.21; P<0.01) as independent factors for disease-free survival (Table III).

*SREBP-1c expression.* Five CH and five cirrhotic liver tissues were selected to analyze the correlation between nuclear PA28γ expression and SREBP-1c gene expression in non-tumor liver tissues. Fig. 4 shows a clear correlation between nuclear PA28γ expression and SREBP-1c gene expression.

## Discussion

The present study shows that non-tumor liver tissues commonly express high levels of nuclear PA28γ protein relative to those of carcinoma tissues. These results are contradictory to those from other studies on other types of cancer, such as thyroid carcinoma; the nuclear PA28γ level was higher in these tumors compared to non-tumor tissues (19). While the exact reason for

Table III. Multivariate analysis of clinicopathological factors for disease-free survival in patients with HCC.

| | n | Relative risk | 95% confidence interval | P-value |
|---|---|---|---|---|
| PA28γ | | | | |
| High | 32 | 2.67 | 1.82-3.22 | <0.01 |
| Low | 14 | | | |
| Portal vein tumor thrombus | | | | |
| Yes | 5 | 2.21 | 1.33-6.38 | 0.023 |
| No | 31 | | | |
| Inflammatory status (HAI score) | | | | |
| Absent-mild (0-3) | 22 | 2.59 | 2.11-3.58 | 0.012 |
| Moderate-severe (>4) | 24 | | | |
| Degree of fibrosis (HAI score) | | | | |
| Absent-moderate (0-2) | 12 | 2.68 | 1.99-7.21 | <0.01 |
| Severe-cirrhosis (>3) | 34 | | | |

HCC, hepatocellular carcinoma; PA28γ, proteasome activator 28γ; HAI, histological activity index.

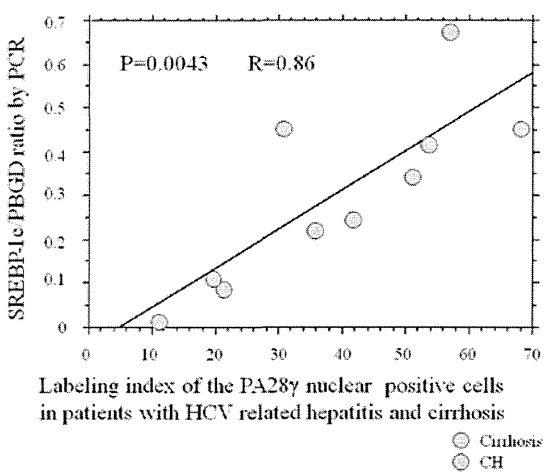


Figure 4. Linear correlation analysis of nuclear PA28γ expression and SREBP-1c gene expression in patients with cirrhosis and chronic hepatitis (CH) (P=0.0043). PA28γ, proteasome activator 28γ; HCV, hepatitis C virus. SREBP-1c, sterol regulatory element binding protein-1c.

the different results is not known at present, it is likely to be related to the type of control tissue used in the present study; the non-tumor tissues were mostly not normal, consisting of HCV-infected CH or cirrhotic tissues. In support of this conclusion, normal liver tissues from patients with metastatic liver tumors from patients with colorectal carcinoma who were negative for HCV/HBV showed low expression of nuclear PA28γ.

In non-neoplastic liver tissues, we found a wide spectrum of nuclear PA28γ expression from normal liver to cirrhosis. Our results also show that active inflammation with hepatitis virus induces nuclear PA28γ in CH and cirrhotic livers (Table II). This is reasonable considering the fundamental action of nuclear PA28γ as a mediator of inflammation. Another mechanism for the high induction of nuclear PA28γ in cirrhosis might be related to the degradation of the HCV core protein by PA28γ and its translocation from the cytoplasm to the nucleus, based on the results of our previous study (10). In fact, nuclear PA28γ-expressing cells had no or faint-to-moderate cytoplasmic PA28γ expression (Fig. 1c and g). Furthermore, the nuclear overexpression could be due to the relatively hypoxic microenvironment in the cirrhotic liver. In this regard, we hypothesized that hypoxia might directly induce PA28γ, which in turn enhances angiogenesis via the enhanced release of a battery of angiogenic growth factors, such as vascular endothelial growth factor (VEGF). Since the VEGF level is increased in cirrhosis (20), it is possible that nuclear PA28γ may improve the ischemic/hypoxic microenvironment in the cirrhotic liver through upregulation of angiogenesis. Although cirrhotic nodules occasionally show p53 mutation and increased telomerase activity (21,22), cirrhosis is not considered a premalignant lesion. However, it is apparent from a number of etiological studies that cirrhosis is a strong risk factor for HCC. In this context, nuclear PA28γ expression in cirrhosis might be a prerequisite for the genesis of premalignant dysplastic nodules or early cancer.

From a clinical point of view, it is interesting to note the correlation between high nuclear PA28γ expression in non-tumor tissues and the relapse of HCC. The prognosis of HCC is generally unfavorable. Although primary tumors are curatively resected, 50-60% of patients develop relapse within 5 years. This is due to either a newly established tumor from the remnant liver, a process termed multicentric carcinogenesis, or recurrence of the original tumor. One possible mechanism for a link between nuclear PA28γ and disease relapse is that high expression of PA28γ in the remnant liver may contribute to carcinogenesis. Nuclear PA28γ expression highly correlated with the presence of active inflammation (P<0.0001). Furthermore, active inflammation in non-tumor tissues has been reported to be associated with relapse of HCC (17,23,24).

In the present study, a clinicopathological survey demonstrated a significant correlation between nuclear PA28γ protein expression and capsular invasion of the cancer tissue. This

finding is in agreement with a recent study that showed increased expression of PA28γ protein during cancer progression and its correlation with PCNA labeling index (19). Thus, the results suggest the possible involvement of PA28γ in HCC progression. Further studies of larger population samples are required to confirm the clinical significance of nuclear PA28γ in HCC. This is particularly important, as the overall survival of patients with high nuclear PA28γ expression was worse than that of those with low expression level (P=0.052) (data not shown).

Also in our series, the labeling index of cytoplasmic expression of PA28γ significantly increased from normal liver to cirrhotic liver (Fig. 2b). Further extended studies are required to determine the importance of cytoplasmic expression of PA28γ in HCC and HCV-related liver.

In conclusion, the present study demonstrates a close correlation between nuclear PA28γ expression in liver tissue and the development and progression of HCC, as well as its possible involvement in HCC relapse. Further studies are required to examine the therapeutic benefits of the suppression of nuclear PA28γ expression in HCV-related CH, cirrhosis or HCC.

## References


1. Montalto G, Cervello M, Giannitrapani L, Dantona F, Terranova A and Castagnetta LA: Epidemiology, risk factors, and natural history of hepatocellular carcinoma. Ann NY Acad Sci 963: 13-20, 2002.
2. Okuda K: Hepatocellular carcinoma: Recent progress. Hepatology 15: 948-963, 1992.
3. Kew MC and Popper H: Relationship between hepatocellular carcinoma and cirrhosis. Semin Liver Dis 4: 136-146, 1984.
4. Ikeda K, Saitoh S, Koida I, Arase Y, Tsubota A, Chayama K, Kumada H and Kawanishi M. A multivariate analysis of risk factors for hepatocellular carcinogenesis: A prospective observation of 795 patients with viral and alcoholic cirrhosis. Hepatology 18: 47-53, 1993.
5. Shiratori Y, Shiina S, Imamura M, *et al*: Characteristic difference of hepatocellular carcinoma between hepatitis B- and C- viral infection in Japan. Hepatology 22: 1027-1033, 1995.
6. Nagasue N, Uchida M, Makino Y, *et al*: Incidence and factors associated with intrahepatic recurrence following resection of hepatocellular carcinoma. Gastroenterology 105: 488-494, 1993.
7. Ikeda K, Saitoh S, Tsubota A, Arase Y, Chayama K, Kumada H, Watanabe G and Tsurumaru M: Risk factors for tumor recurrence and prognosis after curative resection of hepatocellular carcinoma. Cancer 71: 19-25, 1993.
8. Shimada M, Takenaka K, Gion T, *et al*: Prognosis of recurrent hepatocellular carcinoma: a 10-year surgical experience in Japan. Gastroenterology 111: 720-726, 1996.
9. Kumada T, Nakano S, Takeda I, *et al*: Patterns of recurrence after initial treatment in patients with small hepatocellular carcinoma. Hepatology 25: 87-92, 1997.
10. Moriishi K, Mochizuki R, Moriya K, *et al*: Critical role of PA28gamma in hepatitis C virus-associated steatogenesis and hepatocarcinogenesis. Proc Natl Acad Sci USA 104: 1661-1666, 2007.
11. Myers J, Mehta P, Hunter AW, Bernstein SA and Erickson PA. Automated double-label immunohistochemistry. J Surg Pathol 1: 105-113, 1995.
12. Chretien S, Dubart A, Beaupain D, *et al*: Alternative transcription and splicing of the human porphobilinogen deaminase gene result either in tissue-specific or in housekeeping expression. Proc Natl Acad Sci USA 85: 6-10, 1988.
13. Nagel S, Schmidt M, Thiede C, Huhn D and Neubauer A: Quantification of Bcr-Abl transcripts in chronic myelogenous leukemia (CML) using standardized, internally controlled, competitive differential PCR (CD-PCR). Nucleic Acids Res 24: 4102-4103, 1996.
14. Kim KH, Hong SP, Kim K, Park MJ, Kim KJ and Cheong J: HCV core protein induces hepatic lipid accumulation by activating SREBP1 and PPARgamma. Biochem Biophys Res Commun 355: 883-888, 2007.
15. Finke J, Fritzen R, Ternes P, Lange W and Dolken G: An improved strategy and a useful housekeeping gene for RNA analysis from formalin-fixed, paraffin-embedded tissues by PCR. Biotechniques 14: 448-453, 1993.
16. Sasaki Y, Imaoka S, Fujita M, *et al*: Regional therapy in the management of intrahepatic recurrence after surgery for hepatoma. Ann Surg. 206: 40-47, 2007.
17. Ko S, Nakajima Y, Kanehiro H, *et al*: Significant influence of accompanying chronic hepatitis status on recurrence of hepatocellular carcinoma after hepatectomy. Result of multivariate analysis. Ann Surg 224: 591-595, 1996.
18. Sasaki Y, Imaoka S, Masutani S, Ohashi I, Ishikawa O, Koyama H and Iwanaga T: Influence of coexisting cirrhosis on long-term prognosis after surgery in patients with hepatocellular carcinoma. Surgery 112: 515-21, 1992.
19. Okamura T, Taniguchi S, Ohkura T, *et al*: Abnormally high expression of proteasome activator-gamma in thyroid neoplasm. J Clin Endocrinol Metab 88: 1374-1383, 2003.
20. El-Assal ON, Yamanoi A, Soda Y, *et al*: Clinical significance of microvessel density and vascular endothelial growth factor expression in hepatocellular carcinoma and surrounding liver: possible involvement of vascular endothelial growth factor in the angiogenesis of cirrhotic liver. Hepatology 27: 1554-1562, 1998.
21. Raedle J, Oremek G, Truschnowitsch M, Lorenz M, Roth WK, Caspary WF and Zeuzem S: Clinical evaluation of autoantibodies to p53 protein in patients with chronic liver disease and hepatocellular carcinoma. Eur J Cancer 34: 1198-1203, 1998.
22. Kishimoto Y, Shiota G, Kamisaki Y, *et al*: Loss of the tumor suppressor p53 gene at the liver cirrhosis stage in Japanese patients with hepatocellular carcinoma. Oncology 54: 304-310, 1997.
23. Tarao K, Takemiya S, Tamai S, *et al*: Relationship between the recurrence of hepatocellular carcinoma (HCC) and serum alanine aminotransferase levels in hepatectomized patients with hepatitis C virus-associated cirrhosis and HCC. Cancer 79: 688-694, 1997.
24. Ko S, Nakajima Y, Kanehiro H, *et al*: Influence of associated viral hepatitis status on recurrence of hepatocellular carcinoma after hepatectomy. World J Surg 21: 1082-1086, 1996.

PLOS ONE

# Hepatitis B Virus-Specific miRNAs and Argonaute2 Play a Role in the Viral Life Cycle

**C. Nelson Hayes[1,2,3☯], Sakura Akamatsu[1,2,3☯], Masataka Tsuge[3,4], Daiki Miki[1,2,3], Rie Akiyama[1,2,3], Hiromi Abe[1,2], Hidenori Ochi[1,2,3], Nobuhiko Hiraga[1,2,3], Michio Imamura[1,2,3], Shoichi Takahashi[1,2], Hiroshi Aikata[1,3], Tomokazu Kawaoka[1,2,3], Yoshiiku Kawakami[1,2,3], Waka Ohishi[3,5], Kazuaki Chayama[1,2,3]***

**1** Department of Gastroenterology and Metabolism, Applied Life Sciences, Institute of Biomedical & Health Sciences, Hiroshima University, Hiroshima, Japan, **2** Laboratory for Digestive Diseases, Center for Genomic Medicine, RIKEN, Hiroshima, Japan, **3** Liver Research Project Center, Hiroshima University, Hiroshima, Japan, **4** Natural Science Center for Basic Research and Development, Hiroshima University, Hiroshima, Japan, **5** Department of Clinical Studies, Radiation Effects Research Foundation, Hiroshima, Japan

## Abstract

Disease-specific serum miRNA profiles may serve as biomarkers and might reveal potential new avenues for therapy. An HBV-specific serum miRNA profile associated with HBV surface antigen (HBsAg) particles has recently been reported, and AGO2 and miRNAs have been shown to be stably associated with HBsAg in serum. We identified HBV-associated serum miRNAs using the Toray 3D array system in 10 healthy controls and 10 patients with chronic hepatitis B virus (HBV) infection. 19 selected miRNAs were then measured by quantitative RT-PCR in 248 chronic HBV patients and 22 healthy controls. MiRNA expression in serum versus liver tissue was also compared using biopsy samples. To examine the role of AGO2 during the HBV life cycle, we analyzed intracellular co-localization of AGO2 and HBV core (HBcAg) and surface (HBsAg) antigens using immunocytochemistry and proximity ligation assays in stably transfected HepG2 cells. The effect of AGO2 ablation on viral replication was assessed using siRNA. Several miRNAs, including miR-122, miR-22, and miR-99a, were up-regulated at least 1.5 fold ($P<2E-08$) in serum of HBV-infected patients. AGO2 and HBcAg were found to physically interact and co-localize in the ER and other subcellular compartments. HBs was also found to co-localize with AGO2 and was detected in multiple subcellular compartments. Conversely, HBx localized non-specifically in the nucleus and cytoplasm, and no interaction between AGO2 and HBx was detected. SiRNA ablation of AGO2 suppressed production of HBV DNA and HBs antigen in the supernatant.

***Conclusion:*** These results suggest that AGO2 and HBV-specific miRNAs might play a role in the HBV life cycle.

**Citation:** Hayes CN, Akamatsu S, Tsuge M, Miki D, Akiyama R, et al. (2012) Hepatitis B Virus-Specific miRNAs and Argonaute2 Play a Role in the Viral Life Cycle. PLoS ONE 7(10): e47490. doi:10.1371/journal.pone.0047490

**Editor:** Sang-Hoon Ahn, Yonsei University College of Medicine, Republic of Korea

**Received** July 2, 2012; **Accepted** September 11, 2012; **Published** October 16, 2012



**Funding:** This work was supported in part by Grants-in-Aid for scientific research and development from the Ministry of Health, Labor and Welfare and Ministry of Education Culture Sports Science and Technology, Government of Japan. The funders had no role in study design, data collection and analysis, decision to publish, or preparation of the manuscript.

**Competing Interests:** The authors have declared that no competing interests exist.

* E-mail: chayama@hiroshima-u.ac.jp

☯ These authors contributed equally to this work.

## Introduction

Hepatitis B virus (HBV) is a partially double-stranded DNA virus in the Hepadnaviridae family [1]. New therapies are urgently needed for the 350 million chronically infected individuals who face a significantly elevated lifetime risk of cirrhosis and hepatocellular carcinoma [2,3]. Recent insight into the role of non-coding RNAs in the liver has highlighted potential applications of microRNAs (miRNAs) in HBV diagnosis and treatment [4,5,6,7,8,9].

MiRNAs are a class of short non-coding RNAs involved in post-transcriptional gene regulation of multiple pathways [10]. In contrast to messenger RNAs, exosome-free extracellular miRNAs may be nuclease-resistant and remain in circulation for long periods of time by being stably bound to AGO2, a component of the RNA-induced silencing complex [11]. The origin and function of these extracellular miRNAs is unclear, but they may serve as biomarkers for liver injury and cancer [4]. Elucidating the function of hepatic miRNAs in HBV infection is important in the development of strategies to eradicate the virus and assess the risk of HCC. A number of miRNAs have been shown to be up- or down-regulated in HBV infection [4,12,13]. Noting that the defective hepatitis delta virus co-opts HBsAg subviral particles for export, Novellino et al. hypothesized that HBsAg subviral particles might also sequester miRNAs from the liver [5]. Using HBsAg immunoprecipitation, they identified a set of liver-specific and immune regulatory AGO2-bound miRNAs associated with HBsAg.

These reports suggest that AGO2 and a specific subset of miRNAs may participate in HBV replication, either as part of a host anti-HBV defense or as viral strategy to exploit or evade the RISC machinery. In this study, we examined serum miRNA expression in chronic HBV and healthy individuals and found a specific subset of miRNAs that are over-expressed in HBV-positive

patients and in which miR-122 was strongly up-regulated. To determine whether components of the miRNA system are associated with other HBV components, we performed subcellular localization experiments with viral proteins and AGO2.

## Materials and Methods

### Study Subjects

We performed a series of experiments to compare miRNA profiles of healthy and HBV-infected individuals in serum and liver tissue. All patients had chronic hepatitis B and agreed to provide blood samples for a viral hepatitis study. Patient profiles are shown in Table 1. Histopathological diagnosis was made according to the criteria of Desmet et al. [14]. The study protocol conforms to the ethical guidelines of the 1975 Declaration of Helsinki, and all patients provided written informed consent. This study was approved a priori by the ethical committee of Hiroshima University.

### miRNA Expression Levels in Serum

miRNA expression in serum samples was measured using the Toray Industries miRNA analysis system, in which serum miRNA samples were hybridized to 3D-Gene human miRNA ver12.1 chips containing 900 miRNAs (Toray Industries, Inc., Tokyo, Japan). MiRNA gene expression data were scaled by global normalization, and differential expression was analyzed using the limma package in the R statistical framework. Serum was collected from 20 patients with high HBV DNA and HBsAg levels and with either high (>42 IU/l) or low (≤42 IU/l) ALT levels. Serum from the 10 low ALT patients was analyzed as a mixture, whereas serum from each of the 10 high ALT patients was analyzed both separately and as a mixture. For comparison with healthy controls we collected separate mixtures of serum from 10 healthy females and 12 healthy males. Serum samples from each healthy female were also measured separately. All healthy controls were negative for HBsAg, HBcAb, and HCV Ab. For comparison with miRNA expression in hepatocytes, miRNA expression was measured in non-tumor biopsy tissue from an HBV-infected patient and compared to non-cancerous liver tissue samples from two patients without HBV or HCV infection.

**Table 1.** Clinical characteristics of chronic hepatitis B virus patients (n = 248).

| Factor | Value |
|---|---|
| Age | 44 (15–76) |
| Sex (male/female) | 169/77 |
| Alanine aminotransferase (IU/l) | 56 (10–1867) |
| Aspartate aminotransferase (IU/l) | 43.5 (15–982) |
| HBV DNA (IU/ml) | 6.3 (1.8–9.1) |
| Liver fibrosis (1/2/3/4) | 69/102/46/26 |
| Necroinflammatory activity (0/1/2/3/4) | 1/70/127/45/0 |
| γ-glutamyl transpeptidase (IU/l) | 43 (9–459) |
| Alpha-fetoprotein (μg/l) | 6.15 (0–9400) |
| Promthrombin time (s) | 93 (0–146) |
| Albumin (g/dl) | 4.4 (0–5.2) |
| Platelets (x$10^4$/$mm^3$) | 16.75 (1–36) |
| HBsAg (IU/l) | 2765 (0.05–239000) |
| HBeAg (−/+) | 115/127 |
| HBeAb (−/+) | 113/128 |

Continuous variables are shown as median and range, and categorical variables are shown as counts.
Fibrosis and necroinflammatory activity were scored according to the criteria of Desmet et al. [14].
doi:10.1371/journal.pone.0047490.t001

### Quantitative Real-time Polymerase Chain Reaction miRNA Analysis

Using real-time polymerase chain reaction (RT-PCR) we measured the expression of 19 miRNAs in serum from 248 patients with chronic HBV infection and from 10 healthy females and 12 healthy males. Circulating microRNA was extracted from 300 μl of serum samples using the mirVana PARIS Kit (Ambion, Austin, TX) according to the manufacturer's instructions. RNA was eluted in 80 μl of nuclease free water and reverse transcribed using TaqMan MicroRNA Reverse Transcription Kit (Life Technologies Japan, Tokyo, Japan). *Caenorhabditis elegans* miR-238 (cel-miR-238) was spiked to each sample as a control for extraction and amplification steps. The reaction mixture contained 5 μl of RNA solution, 2 μl of 10× reverse transcription buffer, 0.2 μl of 100 mM dNTP mixture, 4 μl of 5× RT primer, 0.25 μl of RNase inhibitor and 7.22 μl of nuclease free water in a total volume of 20 μl. The reaction was performed at 16°C for 30 min followed by 42°C for 30 min. The reaction was terminated by heating the solution at 85°C for 5 min. MiRNAs were amplified using primers and probes provided by Applied Biosystems using TaqMan MicroRNA assays according to the manufacturer's instructions. The reaction mixture contained 12.5 μl of 2× Universal PCR Master Mix, 1.25 μl of 20× TaqMan Assay solution, 1 μl of reverse transcription product and 10.25 μl of nuclease free water in a total volume of 25 μl. Amplification conditions were 95°C for 10 min followed by 50 denaturing cycles for 15 sec at 95°C and annealing and extension for 60 sec at 60°C in an ABI7300 thermal cycler. For the cel-miR-238 assay, a dilution series using chemically synthesized miRNA was used to generate a standard curve that permitted absolute quantification of molecules.

### Pathway Analysis

Target genes of differentially expressed miRNAs were predicted based on agreement among three miRNA prediction tools, miRanda, miRBase, and TargetScan. Gene Set Enrichment Analysis (http://www.broadinstitute.org/gsea) was used to identify significantly over-represented gene ontology (GO) terms among the predicted targets.

### Plasmid Construction

The construction of wild-type HBV 1.4 genome length, pTRE-HB-wt, was described previously [15]. We used pTRE2 vector without pTet-off vector and doxycycline because a sufficient amount of HBV transcript was produced from internal HBV promoters, and transcription from the pTRE2 promoter is negligible under these conditions. The nucleotide sequence of the HBV genome that we cloned into plasmids pTRE-HB-wt was deposited into GenBank under accession number AB206817.

### Cell Culture

HepG2 cells, derived from a human hepatoma cell line, were grown in Dulbecco's modified Eagle's medium (DMEM) supplemented with 10% (v/v) fetal bovine serum at 37°C and under 5% $CO_2$. For the production of stably transfected cell lines, HepG2 cells were transfected with 20μg of the plasmid pTRE-HB-wt by calcium precipitation and the transfected cells were selected with

400μg/ml hygromycin-included DMEM. Sixty colonies were isolated, and clones that were positive for both HBs and HBe antigens were selected. Finally, one cell line named T23 was selected and used for further experiments. T23 cells continuously produced more than 6 log copies/ml of HBV DNA in supernatant over more than 12 months (data not shown).

### Immunocytochemistry

Co-localization between AGO2 and several HBV proteins (HBc, HBs, and HBx) was analyzed using immunocytochemistry, followed by cellular localization assays using antibodies targeting various sub-cellular compartments. HepG2 or T23 cells were seeded in 2-well chamber plates and harvested 48 hours after seeding. The cells were washed with PBS and fixed with 4% (v/v) paraformaldehyde. After fixation, the cells were stained with several primary antibodies (Table S1). The bound antibodies were detected with an Alexa 488-conjugated antibody against rabbit IgG (1:2000) or Alexa 568-conjugated antibody against mouse IgG (1:2000), respectively (Molecular Probes, Eugene, OR). Nuclei were counterstained with 6-diamidino-2-phenylindole (DAPI) (Vector laboratories, Burlingame, CA). The stained cells were examined with a Fluoview FV10i microscope (Olympus, Tokyo, Japan).

### In situ Proximity Ligation Assay

We used proximity ligation assays (PLA) to determine whether AGO2 and HBc physically interact. PLA is a recent method to detect protein-protein interactions using protein-DNA conjugates that can be detected using fluorescence microscopy [16]. PLA improves on traditional immunoassays by directly detecting even weak or transient protein interactions [16]. HepG2 and T23 cells were seeded in 2-well chamber plates and harvested 48 hours after seeding. The cells were washed with PBS and fixed with 4% (v/v) paraformaldehyde. After fixation, the cells were stained with primary antibodies. The primary antibodies used are listed in Table S1. After overnight incubation with primary antibody at 4°C, PLA was performed using Duolink II PLA probe anti-rabbit plus and anti-mouse minus and Duolink II Detection Reagents Orange (Olink, Uppsala, Sweden) following the manufacturer's protocol. Nuclei were counterstained with DAPI. Imaging was performed using a Fluoview FV10i microscope.

### Analysis of Supernatant HBV Production by RNA Interference Against AGO2

To investigate the necessity of AGO2 for HBV production, we performed RNA interference assay using T23 cells that are HepG2 cells stably transfected with the plasmid pTRE-HB-wt. We used Silencer Select Pre-designed siRNA small interfering RNA targeting *AGO2* (#s25932, Ambion, Austin, TX) and Silencer Select Negative Control #1 siRNA for control (Ambion). T23 cells were transfected with one of the siRNA oligonucleotides (10 nM) using Lipofectamine RNAiMAX (Invitrogen, Carlsbad, CA) according to the manufacturer's instructions. To examine the knockdown effect of siRNAs against *AGO2* by real-time quantitative RT-PCR, T23 cells transfected with siRNAs were harvested 72 hours after transfection. Total RNA was isolated using the QuickGene RNA cultured cell kit S (Fujifilm, Tokyo, Japan). One μg of each RNA sample was reverse transcribed with the SuperScript VILO cDNA Synthesis kit (Invitrogen). First-strand complementary DNA (cDNA) was amplified with specific primers for the coding sequence of *AGO2*. The primers were as follows: forward, 5′-CCAGCATACTACGCTCACCT-3′; reverse, 5′-CAGAGTGTCTTGGTGAACCTG-3′. We quantified *AGO2* mRNA with EXPRESS SYBR Green ER qPCR Supermix Universal (Invitrogen) according to the manufacturer's instructions. Amplification and detection were performed using the Mx3000P Multiplex quantitative PCR system (Stratagene, La Jolla, CA). Results were normalized to the transcript levels of the housekeeping reference gene glyceraldehyde-3-phosphate dehydrogenase (*GAPDH*). Three to seven days after transfection, the culture media were collected to examine HBV production in supernatant. HBs antigen was measured quantitatively using the Abbott chemiluminescence immunoassay kit (Abbott Japan, Tokyo, Japan). HBV DNA levels were determined by Cobas TaqMan HBV standardized real-time PCR assay (Roche Molecular Systems, Pleasanton, CA). Results are expressed in log10 international units/ml. We also evaluated viability of cells using the Cell Counting kit-8 (Dojindo Laboratories, Kumamoto, Japan) at 3, 5 and 7 days after transfection, according to the manufacturer's instructions. All assays were performed in triplicate, and the results are expressed as mean ± SD.

### Statistical Analysis

All analyses were performed using the R statistical package (http://www.r-project.org). Continuous variables are reported using the median and range. Moderated t statistics or Mann Whitney U tests were used to detect significant associations, as appropriate, and P-values were adjusted for multiple testing based on the false discovery rate.

## Results

### MiRNA Microarray Results

We performed miRNA microarray analysis to identify HBV-associated differences in serum miRNA profiles between 10 chronic HBV patients and 10 healthy controls (Fig. S1). 26 miRNAs with an absolute log fold change greater than 1.5 were found to be significantly ($P_{FDR} < 0.05$) up-regulated in serum of HBV patients, and 8 miRNAs were significantly down-regulated (Table 2). MiR-122, miR-22, and miR-99a levels were the most strongly up-regulated in serum of HBV-infected patients, and levels of miR-575, miR-125a-3p, and miR-4294 were the most down-regulated. We also examined miRNAs associated with presence of HBe antigen or HBe antibody, but no miRNAs were significant following correction for multiple testing (data not shown).

### Analysis of Serum Sample Mixtures from HBV-infected Patients and Healthy Controls

In addition to individual serum samples, we also examined 4 pooled serum samples as follows: 10 healthy males, 10 healthy females, 10 HBV patients with low ALT levels, and 10 HBV patients with high ALT levels (Fig. S2). In agreement with results from individual analysis, miR-122 and miR-99 levels were significantly higher in serum from HBV serum samples compared to healthy control samples (Table 2). Corresponding results with a log change greater than 1.5 were found for several other miRNAs, including miR-22, miR-642b, miR-125b (up-regulated) and miR-575 and miR-4294 (down-regulated), but results were not significant following correction for multiple testing in the mixture samples due to the small number of samples compared.

### RT-PCR Analysis

Serum levels of 19 miRNAs were analyzed using quantitative RT-PCR analysis of 250 chronic HBV patients and 20 healthy controls. Several miRNAs (miR-122, miR-22, miR-99a, miR-720, miR-125b, and miR-1275) were significantly up-regulated in

**Table 2.** Top 10 up- or down-regulated serum miRNAs associated with chronic HBV infection.

| Sample | Direction | miRNA | logFC | AveExpr | t | P | $P_{FDR}$ |
|---|---|---|---|---|---|---|---|
| Serum | Up | hsa-miR-122 | 5.97 | 9.09 | 12.84 | 3.27E−12 | 3.06E−09 |
| | | hsa-miR-99a | 2.59 | 6.20 | 10.73 | 2.11E−10 | 2.19E−08 |
| | | hsa-miR-22 | 2.49 | 9.55 | 10.47 | 2.10E−10 | 2.19E−08 |
| | | hsa-miR-191 | 2.19 | 8.42 | 11.87 | 1.68E−11 | 3.93E−09 |
| | | hsa-miR-642b | 2.03 | 10.07 | 9.93 | 5.92E−10 | 4.26E−08 |
| | | hsa-miR-125b | 1.95 | 5.99 | 8.72 | 9.91E−09 | 4.21E−07 |
| | | hsa-miR-486-3p | 1.79 | 9.09 | 8.01 | 3.19E−08 | 9.95E−07 |
| | | hsa-miR-378 | 1.78 | 5.97 | 9.94 | 9.00E−10 | 6.02E−08 |
| | | hsa-miR-320d | 1.70 | 7.19 | 7.88 | 4.25E−08 | 1.21E−06 |
| | | hsa-miR-23b | 1.69 | 8.99 | 7.62 | 7.64E−08 | 1.93E−06 |
| | Down | hsa-miR-575 | −2.10 | 8.35 | −10.00 | 5.20E−10 | 4.05E−08 |
| | | hsa-miR-125a-3p | −1.99 | 7.22 | −11.91 | 1.56E−11 | 3.93E−09 |
| | | hsa-miR-4294 | −1.75 | 11.82 | −11.37 | 4.07E−11 | 7.63E−09 |
| | | hsa-miR-92a-2* | −1.64 | 11.03 | −7.70 | 6.36E−08 | 1.75E−06 |
| | | hsa-miR-1202 | −1.59 | 8.60 | −12.41 | 6.72E−12 | 3.14E−09 |
| | | hsa-miR-30c-1* | −1.31 | 6.29 | −8.66 | 1.12E−08 | 4.35E−07 |
| | | hsa-miR-1275 | −1.19 | 9.91 | −7.50 | 1.00E−07 | 2.35E−06 |
| | | hsa-miR-3197 | −1.05 | 11.46 | −8.58 | 9.24E−09 | 4.21E−07 |
| | | hsa-miR-1908 | −1.03 | 13.75 | −9.05 | 3.49E−09 | 2.04E−07 |
| Mixture | Up | hsa-miR-122 | 6.80 | 9.09 | 20.51 | 1.09E−06 | 0.001 |
| | | hsa-miR-99a | 2.58 | 6.34 | 9.32 | 9.80E−05 | 0.037 |
| | | hsa-miR-22 | 2.07 | 8.60 | 3.16 | 0.020 | 0.528 |
| | | hsa-miR-125b | 2.03 | 6.29 | 5.09 | 0.002 | 0.264 |
| | | hsa-miR-1915* | 1.80 | 8.32 | 6.24 | 0.001 | 0.158 |
| | | hsa-miR-3648 | 1.69 | 14.16 | 5.06 | 0.002 | 0.264 |
| | | hsa-miR-642b | 1.64 | 9.82 | 4.49 | 0.004 | 0.377 |
| | | hsa-miR-1288 | 1.39 | 6.43 | 3.56 | 0.012 | 0.528 |
| | | hsa-miR-325 | 1.30 | 4.91 | 2.87 | 0.047 | 0.586 |
| | | hsa-miR-486-3p | 1.29 | 8.98 | 3.87 | 0.009 | 0.480 |
| | Down | hsa-miR-575 | −1.95 | 8.43 | −6.38 | 0.001 | 0.158 |
| | | hsa-miR-4294 | −1.79 | 11.95 | −5.99 | 0.001 | 0.158 |
| | | hsa-miR-654-3p | −1.35 | 5.36 | −2.99 | 0.042 | 0.569 |
| | | hsa-miR-1202 | −1.24 | 8.52 | −3.97 | 0.008 | 0.480 |
| | | hsa-miR-1237 | −1.06 | 7.52 | −3.10 | 0.022 | 0.531 |
| | | hsa-miR-744 | −1.03 | 9.51 | −2.91 | 0.028 | 0.545 |

Expression levels were compared using moderated t-statistics, and P-values were corrected for multiple testing using the false discovery rate.
logFC: log2 fold-change between patients with chronic HBV infection relative to healthy individuals.
AveExpr: The average log2 expression level for each miRNA over all samples.
t: moderated t-statistic for patients with chronic HBV infection compared to healthy individuals P for each miRNA.
P: uncorrected P-value for t-test.
$P_{FDR}$: P-value adjusted for multiple testing based on the false discovery rate.
doi:10.1371/journal.pone.0047490.t002

serum from HBV-infected patients (Table 3). Agreement of microarray and RT-PCR results was strongest for up-regulation of miR-122, miR-22, and miR-125b in serum of HBV patients. To determine whether there is a linear relationship between HBV markers and HBV-associated miRNAs, we analyzed the correlation between HBsAg and 6 up-regulated miRNAs. MiR-122, miR-99a, and miR-125b levels were found to be significantly correlated with HBsAg levels with $R^2>0.5$ (Fig. S3). These three miRNAs were also significantly correlated with HBV DNA titers, with $R^2$ of about 0.4 (Fig. S4). MiR-122 and miR-22 were significantly but diffusely associated with serum ALT levels ($R^2>0.2$; Fig. S5). To identify miRNAs associated with different phases of HBV infection, we also analyzed the 6 significantly up-regulated miRNAs with respect to the presence of HBe antigen and antibody. MiR-122, miR-99a, miR-720, and miR-125b were each highly significantly elevated in chronic HBV patients who were positive for the HBe antigen (P<4.0E−07; Fig. S6). Similarly, each miRNA was significantly elevated in chronic HBV patients who were negative for the HBe antibody (P<9.1E−05; Fig. S7).

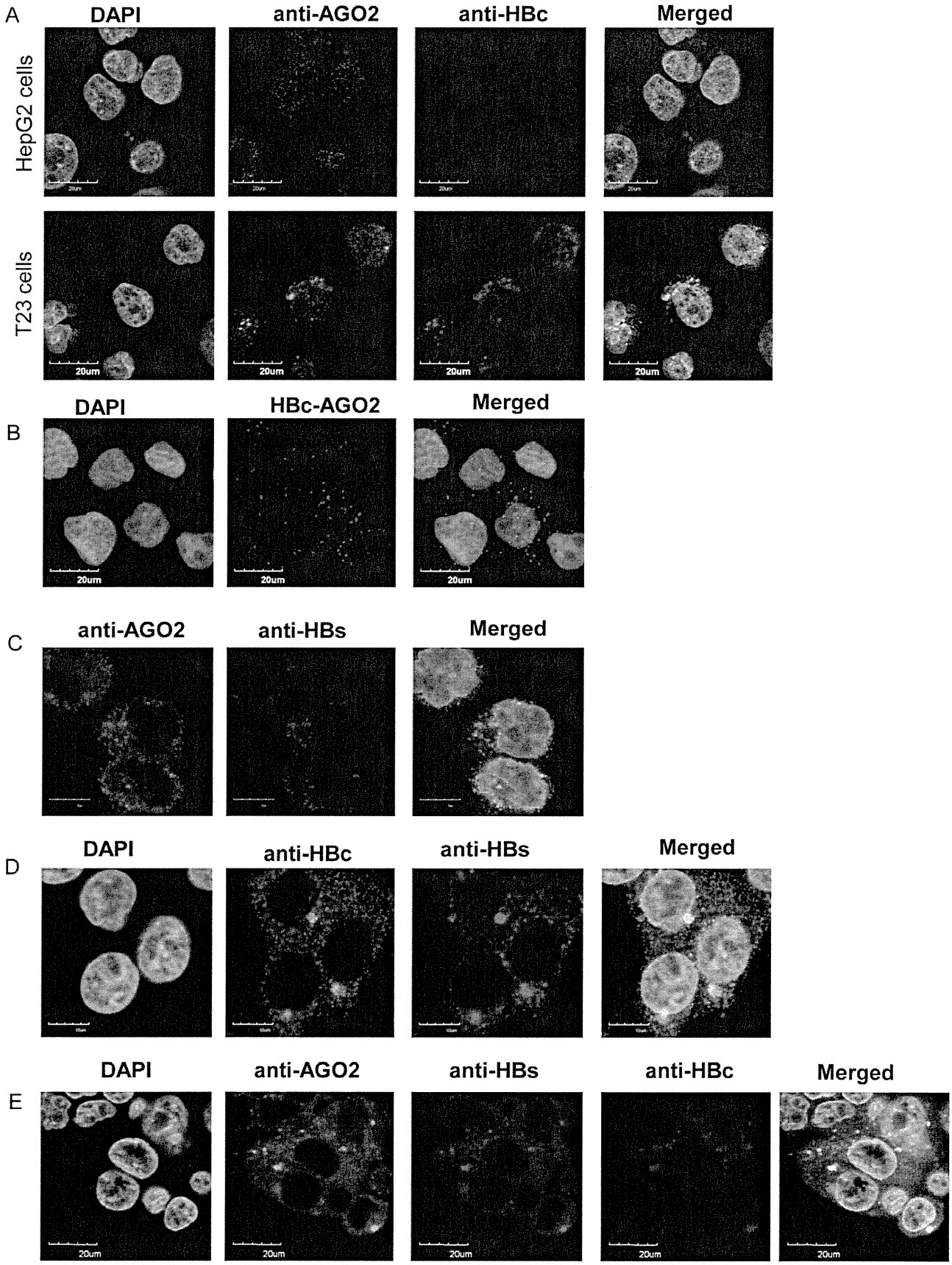
A
DAPI
anti-AGO2
anti-HBc
Merged
HepG2 cells
T23 cells
20um
B
DAPI
HBc-AGO2
Merged
C
anti-AGO2
anti-HBs
Merged
D
DAPI
anti-HBc
anti-HBs
Merged
E
DAPI
anti-AGO2
anti-HBs
anti-HBc
Merged

**Figure 1. Co-localization of HBcAg and HBsAg with AGO2 in stably transfected T23 cells.** A) Anti-AGO2 and anti-HBc staining overlapped in stably transfected T23 cells, but not in HepG2 control cells, suggesting an interaction between HBc and AGO2. B) HBc-AGO2 was detected in T23 but not HepG2 cells using proximity ligation assays (PLA), suggesting a protein-protein interaction between HBcAg and AGO2. C) Overlap of anti-AGO2 and anti-HBs staining suggests co-localization of HBs and AGO2. D) Anti- HBc, and anti-HBs staining overlapped in T23 cells, which may indicate that HBc and HBs co-localize. E) Overlap of anti-AGO2, anti-HBc, and anti-HBs staining in T23 cells suggests that all three proteins may co-localize.
doi:10.1371/journal.pone.0047490.g001

## Pathway Analysis

Predicted gene targets of up-regulated miRNAs were most strongly associated with the GO term PROTEIN_TYROSINE_PHOSPHATASE_ACTIVITY (P = 5.24E−3), and down-regulated miRNAs were associated with the term POSITIVE_REGULATION_OF_JNK_ACTIVITY (P 9.47e−4). Predicted target genes associated with phosphatase activity and dephosphorylation included MTMR3, PTPN18, DUSP5, PTPN2, DUSP2, and PPP1CA.

## MiRNA Expression in Liver Biopsy Samples

We compared miRNA expression in non-cancerous liver biopsy samples from a patient with chronic HBV to two uninfected patients (Table S2, Fig. S8). MiRNA levels were highly correlated between liver tissue and serum in all patients (P = <0.001; $R^2 = 0.57$), including the top HBV-associated miRNAs identified by microarray and RT-PCR analysis in this study.

## Co-localization of HBcAg and HBsAg with AGO2

Using immunocytochemistry and PLA analysis, we found that HBV core protein and AGO2 co-localized within T23 cells (Fig. 1A–B), suggesting a potential protein-protein interaction between HBcAg and AGO2. AGO2 also co-localized with HBs in T23 cells (Fig. 1C), indicating a potential interaction between HBs and AGO2. Overlap between anti-HBc and anti-HBs staining (Fig. 1D) and between anti-AGO2, anti-HBc, and anti-HBs (Fig. 1E) suggests that these three proteins may co-localize. No overlap was observed between anti-AGO2 and anti-HBx staining in HepG2 cells transfected with HBx expression plasmid (p3FLAG-HBx) nor in control cells, suggesting that HBx does not interact with AGO2 (data not shown).

## Subcellular Localization

We also examined HBcAg sub-cellular localization using immunocytochemistry and PLA analysis and found that HBcAg localized to several intracellular compartments, including the ER, autophagosomes, endosomes, and Golgi (Fig. 2). No evidence was found for interaction with mitochondria (data not shown). Using immunocytochemistry, HBsAg was also found to localize diffusely to several intracellular compartments, including the ER, endosomes, autophagosomes, Golgi, mitochondria, processing bodies, multi-vesicular bodies, and the nuclear envelope (Fig. 3). HBx localized non-specifically in the nucleus and cytoplasm, and no sub-cellular location could be ascertained (Fig. S9).

## RNA Interference against AGO2

Antisense RNA directed against AGO2 strongly suppressed AGO2 expression (Fig. 4A) and resulted in lower HBV DNA (Fig. 4B) and HBsAg (Fig. 4C) levels in the supernatant. Cell viability was not significantly reduced (Fig. 4D).

# Discussion

In this study, we report a set of miRNAs that were up-regulated in serum of HBV infected individuals compared to healthy

**Table 3.** Quantitative RT-PCR results of selected miRNAs associated in serum of chronic HBV patients.

| Factor | Total (n = 270) | HBV (n = 248) | Healthy (n = 22) | P |
|---|---|---|---|---|
| hsa-miR-122/cel-miR-238 | 0.1513 (0.0068–2.5) | 0.1635 (0.0068–2.5) | 0.02074 (0.013–0.04) | 1.19E−13 |
| hsa-miR-22/cel-miR-238 | 0.3 (0.06–1.7) | 0.3028 (0.06–1.7) | 0.2252 (0.11–0.48) | 6.35E−03 |
| hsa-miR-99a/cel-miR-238 | 0.09121 (0.0046–2.4) | 0.102 (0.0086–2.4) | 0.0136 (0.0046–0.051) | 4.61E−12 |
| hsa-miR-720/cel-miR-238 | 0.1206 (0.024–3.7) | 0.1345 (0.031–3.7) | 0.04274 (0.024–0.12) | 8.93E−11 |
| hsa-miR-125b/cel-miR-238 | 0.09732 (0.0066–3.1) | 0.1131 (0.0066–3.1) | 0.02255 (0.0066–0.05) | 1.92E−11 |
| hsa-miR-1275/cel-miR-238 | 0.4842 (0.099–1.6) | 0.5046 (0.099–1.6) | 0.4044 (0.24–0.6) | 0.010781066 |
| hsa-miR-1826/cel-miR-238 | 0.5023 (0.14–4.6) | 0.5583 (0.26–4.6) | 0.33 (0.14–1.4) | 7.23E−03 |
| hsa-miR-1308/cel-miR-238 | 2.831 (1.1–6.9) | 2.578 (1.1–6.9) | 3.113 (2.3–4.7) | 0.223164946 |
| hsa-miR-923/cel-miR-238 | 3.8 (1.8–9.6) | 4.141 (1.8–9.6) | 3.01 (2–5) | 0.104331611 |
| hsa-miR-1280/cel-miR-238 | 1.089 (0.36–5) | 1.332 (0.6–5) | 0.5275 (0.36–0.8) | 1.06E−05 |
| hsa-miR-26a/cel-miR-238 | 1.221 (0.34–3.4) | 1.221 (0.34–3.4) | 1.231 (0.82–2.4) | 0.532171224 |
| hsa-let-7a/cel-miR-238 | 0.9608 (0.2–2.5) | 0.9211 (0.2–2.5) | 1.074 (0.71–1.9) | 0.235258945 |
| hsa-let-7f/cel-miR-238 | 1.134 (0.052–2.6) | 1.126 (0.052–2.6) | 1.143 (0.8–1.7) | 0.639411853 |
| hsa-let-7d/cel-miR-238 | 1.147 (0.35–1.9) | 1.106 (0.35–1.8) | 1.231 (0.73–1.9) | 2.88E−01 |
| hsa-miR-638/cel-miR-238 | 1.23 (0.3–7) | 1.082 (0.3–7) | 1.366 (0.68–4) | 0.288244047 |
| hsa-miR-1908/cel-miR-238 | 1.369 (0.45–3.2) | 1.357 (0.45–1.9) | 1.447 (0.7–3.2) | 0.370765019 |
| hsa-miR-34a/cel-miR-238 | 0.07502 (0.013–1.2) | 0.108 (0.026–1.2) | 0.02738 (0.013–0.044) | 1.41E−05 |
| hsa-miR-886-5p/cel-miR-238 | 1.627 (0.54–3.6) | 1.773 (0.54–3.6) | 1.55 (0.97–2.7) | 0.478520977 |

Expression levels were compared using the Mann-Whitney U test.
doi:10.1371/journal.pone.0047490.t003

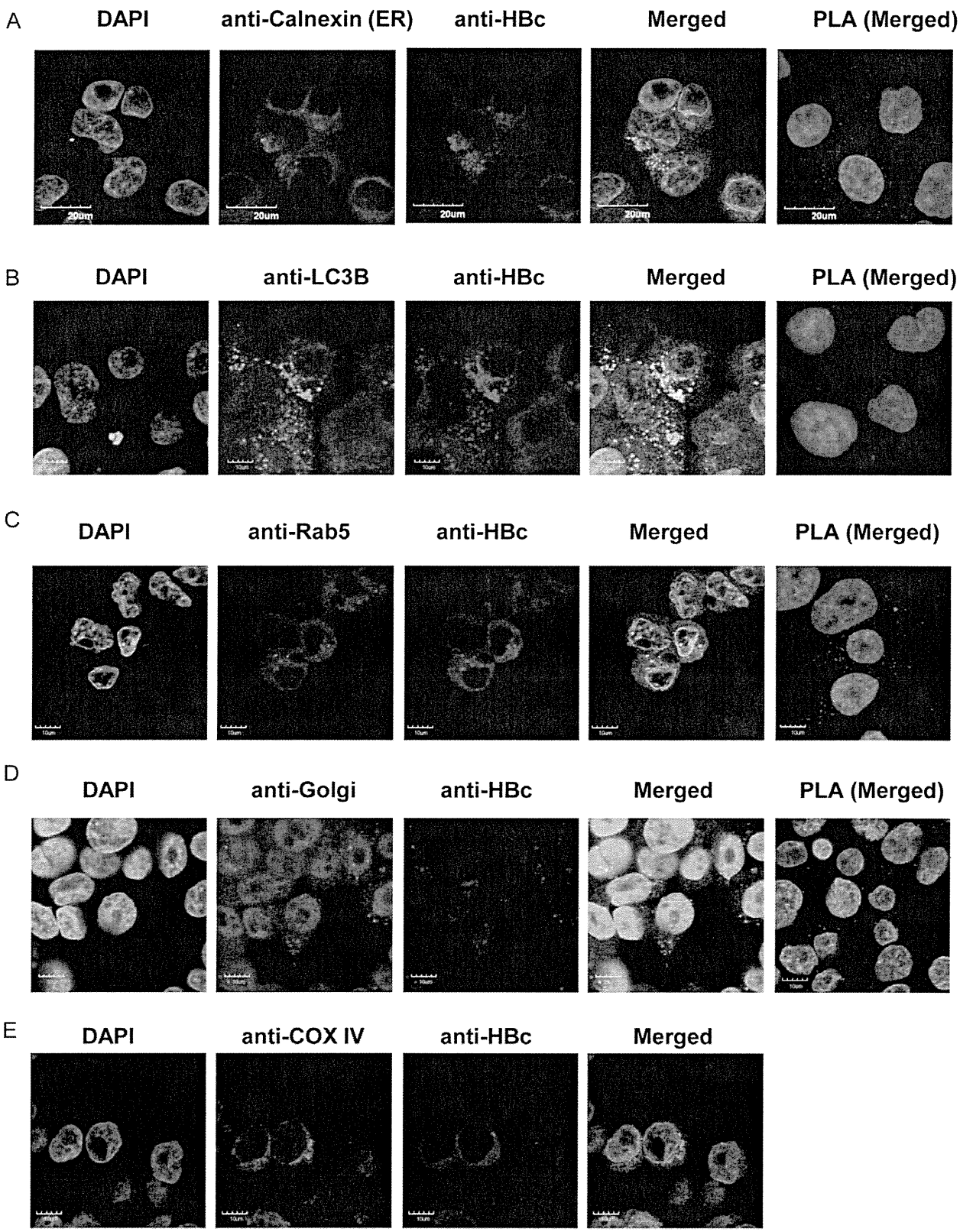


**Figure 2. Interactions between HBc and HBs.** A) Co-localization of anti-HBc and anti-Calnexin staining by immunocytochemistry and PLA analysis indicate that HBc probably localizes in the ER. Overlap with B) anti-LC3B, C) anti-Rab5, and D) anti-Golgi staining suggests that HBc probably also localizes in autophagosomes, endosomes, and Golgi, respectively. E) However, no overlap was observed with anti-COX IV staining, indicating that HBc probably does not localize at mitochondria.
doi:10.1371/journal.pone.0047490.g002

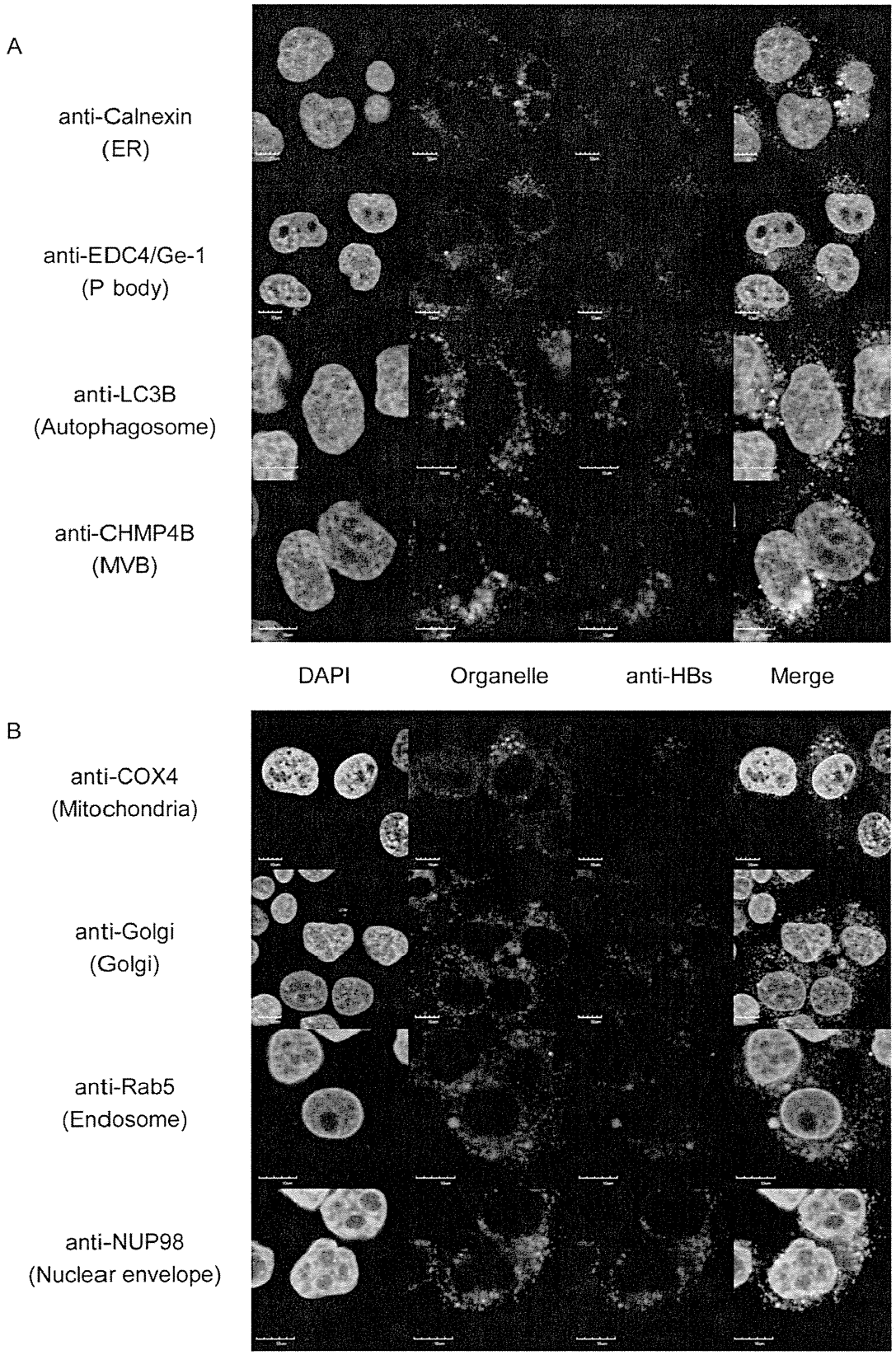


**Figure 3. HBsAg localization.** A) Co-localization of anti-HBs suggests that HBs localizes in the ER, processing bodies, autophagosomes, and multivesicular bodies, B) and more diffusely in mitochondria, Golgi, endosomes, and at the nuclear envelope.
doi:10.1371/journal.pone.0047490.g003

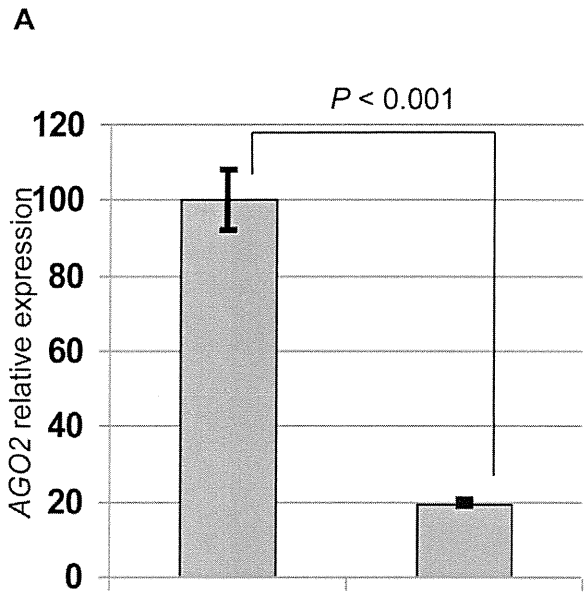
A
P < 0.001
AGO2 relative expression
120
100
80
60
40
20
0
si-control
si-AGO2

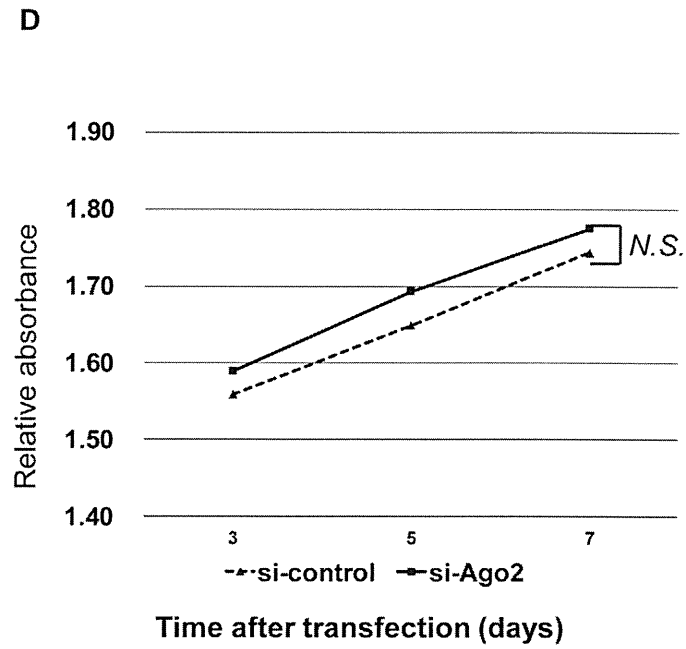
D
Relative absorbance
1.90
1.80
1.70
1.60
1.50
1.40
N.S.
3
5
7
si-control
si-Ago2
Time after transfection (days)

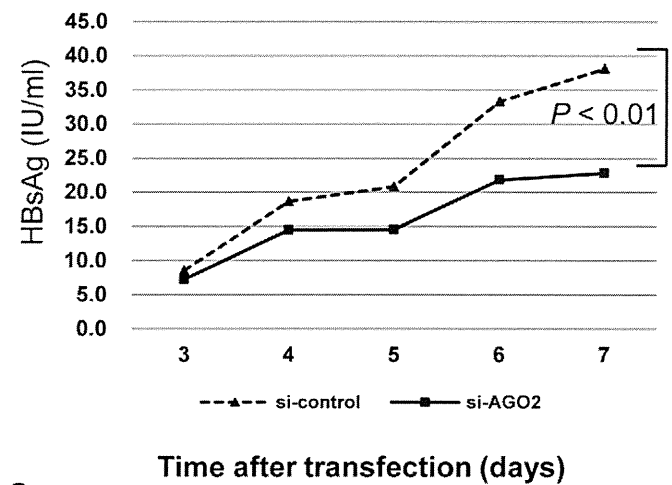
B
HBsAg (IU/ml)
45.0
40.0
35.0
30.0
25.0
20.0
15.0
10.0
5.0
0.0
P < 0.01
3
4
5
6
7
si-control
si-AGO2
Time after transfection (days)

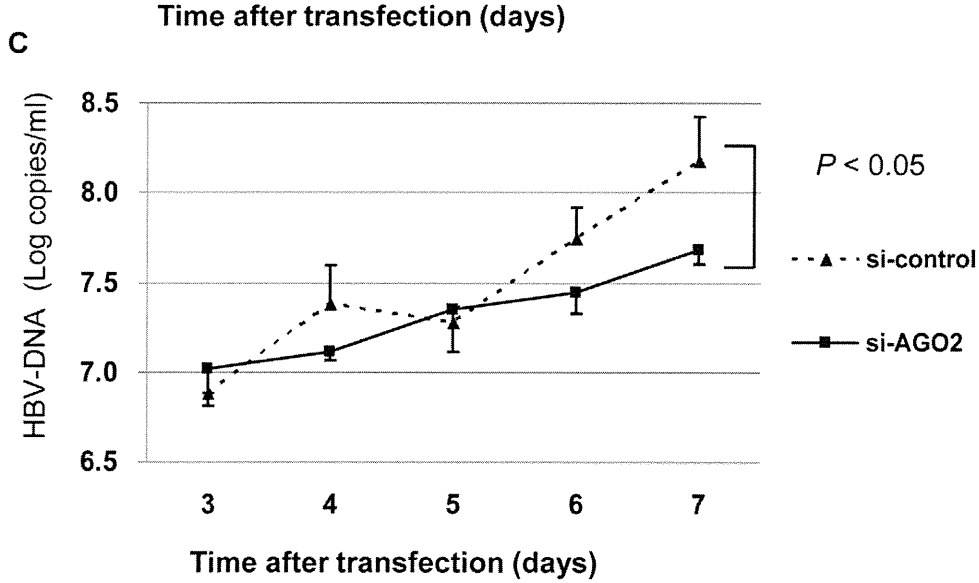
C
HBV-DNA (Log copies/ml)
8.5
8.0
7.5
7.0
6.5
P < 0.05
si-control
si-AGO2
3
4
5
6
7
Time after transfection (days)